Design and Development of a Passive Prosthetic Ankle

by

Sandesh Ganapati Bhat

A Thesis Presented in Partial Fulfillment
of the Requirements for the Degree
Master of Science

Approved November 2017 by the
Graduate Supervisory Committee:

Sangram Redkar, Chair
Hamidreza Marvi
Hyunglae Lee
Thomas Sugar

ARIZONA STATE UNIVERSITY

December 2017

ABSTRACT

In this work, different passive prosthetic ankles are studied. It is observed that complicated designs increase the cost of production, but simple designs have limited functionality. A new design for a passive prosthetic ankle is presented that is simple to manufacture while having superior functionality. This prosthetic ankle design has two springs: one mimicking Achilles tendon and the other mimicking Anterior-Tibialis tendon. The dynamics of the prosthetic ankle is discussed and simulated using Working model 2D. The simulation results are used to optimize the springs stiffness. Two experiments are conducted using the developed ankle to verify the simulation It is found that this novel ankle design is better than Solid Ankle Cushioned Heel (SACH) foot. The experimental data is used to find the tendon and muscle activation forces of the subject wearing the prosthesis using OpenSim. A conclusion is included along with suggested future work.

ACKNOWLEDGMENTS

TABLE OF CONTENTS

LIST OF FIGURES

LIST OF TABLES

CHAPTER 1

INTRODUCTION

This thesis presents a new design of a passive prosthetic ankle. The motivation for this thesis will be discussed in this chapter along with the history of passive prostheses, research on passive ankle devices, and the problem statement.

1.1 Motivation

There are 185,000 new leg amputations each year in the USA alone (MF and LJ. 1998). The major reasons for leg amputations are vascular diseases (54%), trauma (45%), and cancer (less than 1%), to mention a few (KathrynZiegler-Graham, et al. 2008). There is a dire need for prosthetic devices that operate as effectively as human limbs. Existing ankle prostheses either require external power or are not very efficient. High cost is also one of the problems. This warrants the need for an efficient, low/ no power consuming, cheap prosthetic ankle. To develop such an ankle, it is necessary to study the history of prostheses.

1.2 History

1.2.1. Pre 20$^{\text{th}}$ Century

The technology present before the 20$^{\text{th}}$ Century was very crude and couldn't be used to create a prosthesis capable of normal gait. The earliest known prosthesis was discovered in Cairo, Egypt on a mummified body. It is a simple toe prosthesis and is called "The Cairo Toe" (Garber 2013).

Later in the 19$^{\text{th}}$ century, scientists and engineers were developing prosthetic legs that were popular and widely used. A lower limb prosthesis by Pieter Verduyn created in 1659 was well known for its non-locking knee (Go 2015)

Figure 1. The Cairo Toe (Garber 2013)

While in 1800, James Potts designed a prosthesis with an articulated foot controlled by artificial tendons connecting the knee and the ankle. It became popular as the "Selpho Leg" in the USA in 1839. Benjamin Palmer made some changes to the Selpho Leg In 1846. He added an anterior spring and made the leg look more real by concealing the tendons. These prostheses paved way for newer and better prosthetic devices in the 20th century.

1.2.2. Post 20th Century

American scientists started developing newer prosthesis in the 20th century due to the high number of amputations during the U.S. Civil War.

Figure 2. Prosthetic Leg Developed by Pieter Verduyn (Go 2015)

Figure 3. Jaipur Foot Without the Calf Stump (Jaipurfoot.org 2016)

Also, the amputees of World War II were dissatisfied with their prosthesis. Technologically advanced and efficient prostheses were desired. This led to the development of powered as well as passive prosthesis. Some of the passive prosthesis are discussed below:

Jaipur Foot:

The Jaipur foot (Figure 3) is a passive prosthesis developed by Ram Chander Sharma in 1968. It is a very simple prosthesis without any moving parts. It is easy to manufacture and to fit as it is made from polyurethane. Made completely out of rubber, it can bend in multiple ways to provide a good gait, which is still far from the normal gait. Its greatest advantage is its cost which is only 45 USD. (Jaipur Leg 2017)
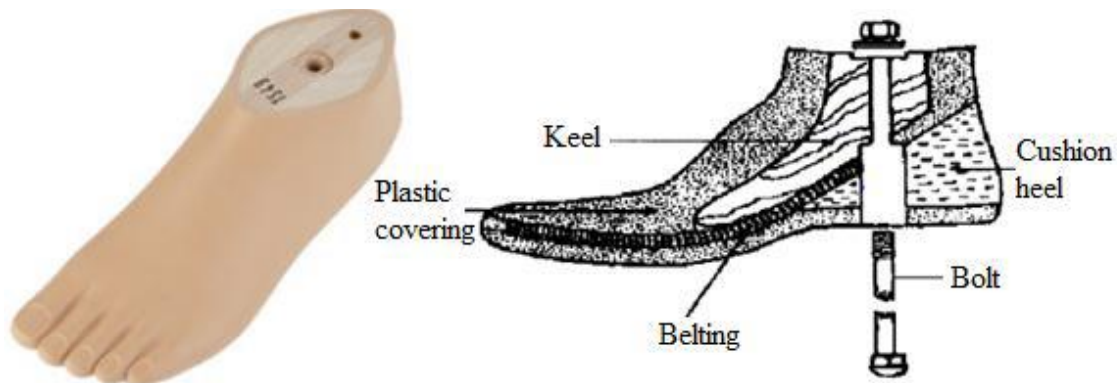
Figure 4. SACH Foot (Zeng 2013)

Solid Ankle Cushion Heel (SACH):

Like the Jaipur foot, SACH is a passive prosthetic ankle. It is a well-known prosthesis due to its common and easy design and its usability for amputees with low activity requirements. It is primarily built out of wood and rubber. Its components are a wooden keel, rubber heel, belting that separates the two

materials and a plastic cover to keep everything in place as shown in Figure 4. (Zeng 2013)

Össur Pro-Flex:

A step above SACH, Össur's Pro-Flex is a commercial passive ankle currently on the market. It delivers a push off generated by mechanical levers. The center of pressure moves across the base of the foot in a natural fashion mimicking a human ankle. This allows the user to perform a desirable gait (Ossur Americas 2017).

Figure 5. Össur's Pro-Flex Ankle

All the above prostheses provide the user with an option to improve their lifestyle after amputation. These devices are a result of the hard work done by researchers and innovators across the world. Hence, it is important to discuss the research done by some of the leading minds in the field of prosthesis.

1.3 Past Research on Passive Prosthetic Ankles

Hansen et al. (Hansen, Childress and Miff 2004) studied the characteristics of human gait on inclines. They studied the roll-over shapes of able bodied human beings over level ground, 5-degree ramp and 10-degree ramp. Two types of roll over shapes were studied: Ankle-Foot roll-over shape (AF) and Knee-Ankle-Foot roll over shape (KAF). After performing their tests and experiments, they found that AF roll-over shapes worked well for uphill walking but KAF rollover shapes were better with both type of inclinations. They concluded that proper ankle actuation improves uphill walking and efficient knee actuation is beneficial for downhill walking.

Vrieling et al. did something similar and studied how amputee's gait adapts to inclines. The study included a variety of test subjects (seven trans-femoral amputees, twelve trans-tibial amputees and ten able-bodied people). This was different than what Hansen et al. did as amputee gait was studied along with able bodied gait. The data agreed with Hansen et al.'s result that knee flexion is important during uphill or downhill walking. (Vrieling, et al. 2008)

Similarly, Williams et al. developed a prosthetic ankle capable of adapting to the walking surface (Williams, Hansen and Gard 2009). Their design used a locking cam mechanism which locked depending on gait transitions. It had three compliant components that defined the overall dynamics of the ankle. The ankle prototypes were tested on three test subjects and were compared with their own daily use prosthetic devices. Figure 6 shows the CAD model of William et al.'s design.
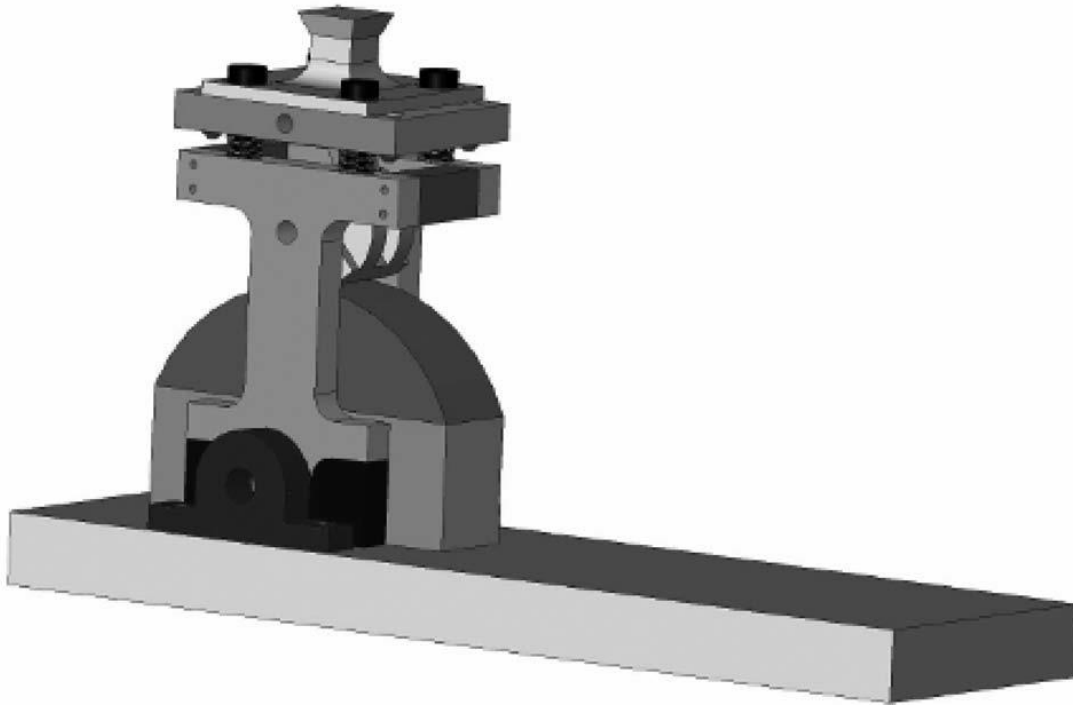
Figure 6. CAD Model of Wiliam Et Al.'S Ankle (Williams, Hansen and Gard 2009)

Later in 2012, Brackx et al. designed a prosthetic ankle with extended push off capability (Brackx, et al. 2012). They observed that the prostheses during that period mostly consisted of springs, which couldn't provide a good push off. So, they came up with a novel idea with planetary gears, locking mechanism and springs. Figure 7 shows the CAD model of their planetary gear mechanism. They experimented on a transfemoral amputee and collected data. Their experiments showed that their design worked and there was energy release during the entirety of the push-off phase of the gait cycle.
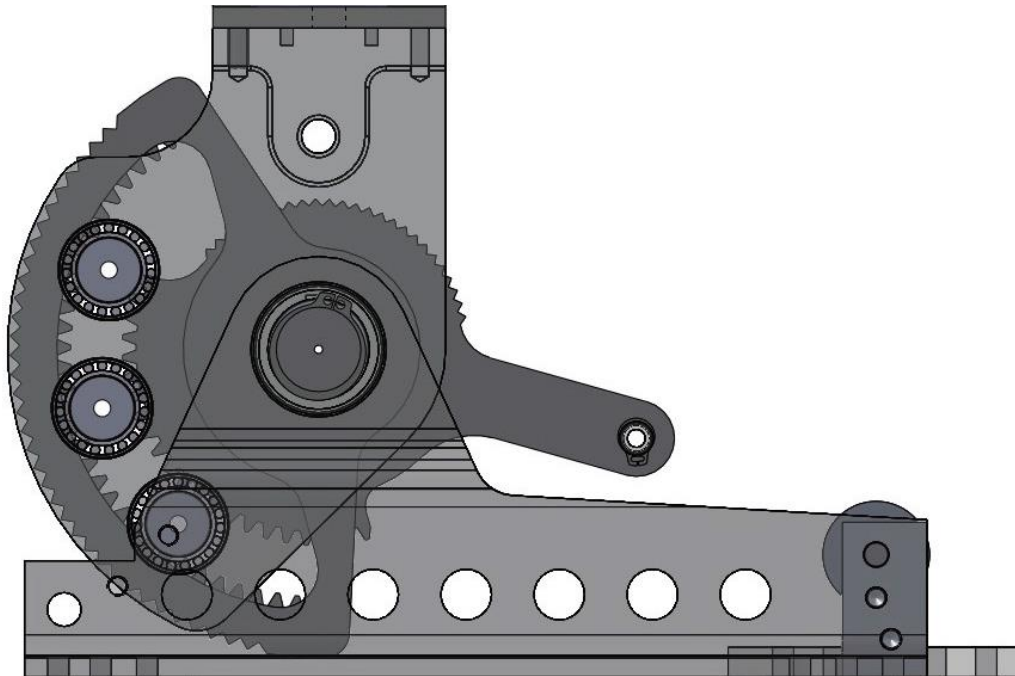
Figure 7. Planetary Gear Mechanism in Brackx Et Al.'S Paper (Brackx, et al. 2012)

In the same vein as Brackx et al., Mooney and his team found that the existing prosthetic ankles at their time were incapable of providing the amputee with "biologically realistic" ankle torque and angles (Mooney, Lai and Rouse 2014). They developed a quasi-passive ankle with pneumatic components. They compared their ankle with a passive ESR prosthetic foot. Their results suggested more tuning of their parameters is required.

Recently, Nickel et al. (Nickel, Sensinger and Hansen 2014) developed a passive prosthetic ankle that automatically adapted to the ground's inclination (Figure 8). All this was achieved using a cam mechanism that changed the equilibrium point that allowed the flexible foot to store energy during plantarflexion. They tested their ankle prototype on inclines ranging from -10 to 10 degrees. The test subjects experienced ease during downhill decent but uphill ascent was difficult. All the test data was compared to the prosthesis that the test subjects used daily. Nickel et al. outlined user

experience while wearing the prosthesis. Their experiments showed that the subjects felt less fatigued when using the prototype.
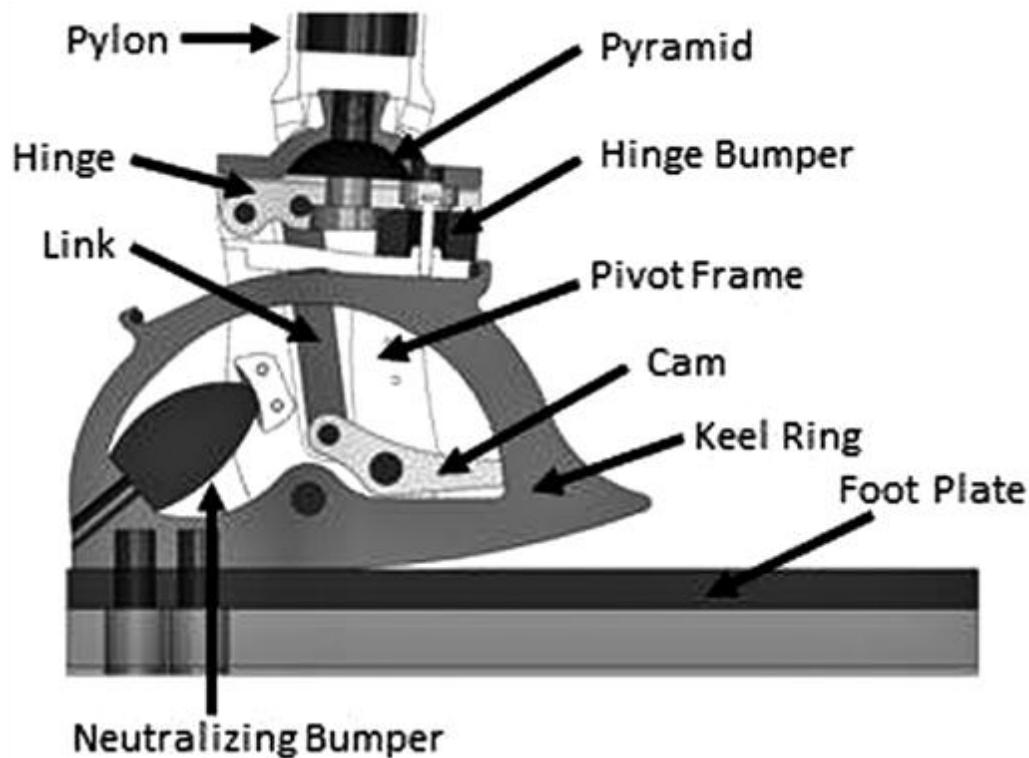
Figure 8. Nickel Et Al.'S Ankle Design (Nickel, Sensinger and Hansen 2014)

In the current year, Amiot et al. (Amiot, et al. 2017) developed a passive hydraulic design (as shown in Figure 9) for a prosthetic ankle as a proof of concept. Their design allowed the ankle to change foot angles according to the slopes. This design had a flexible foot and spring to store energy during plantarflexion. The hydraulic circuit equalized pressure when the foot was flat on the ground. The hydraulic losses in the system were compensated by the energy stored in the flexible foot keeping the system efficient and stable.

Shortly after Amiot and his team, Nguyen et al. designed and developed a revised iteration of their prosthetic ankle that was compliant in 6 degrees of freedom (Nguyen, Dao and Huang 2017). It was a sheet of metal bent to the shape of an ankle as shown

9

in Figure 10. They analyzed the design to check for stress characteristics and found that the design had a better strain energy storage when compared to the previous iterations. They didn't test the ankle in real life experiments where the ankle behavior could be different.

All the articles discussed above lead to the fact that many researchers have tried to design a bionic passive prosthesis. Their research was an inspiration and it was necessary to consider their successes and failures. A very important term that was used in all the articles mentioned above was 'human gait'. Human gait is defined as any movement caused by the human limbs. It becomes important to technically define normal human gait to design and develop a prosthesis. Normal gait will be discussed in the next section.
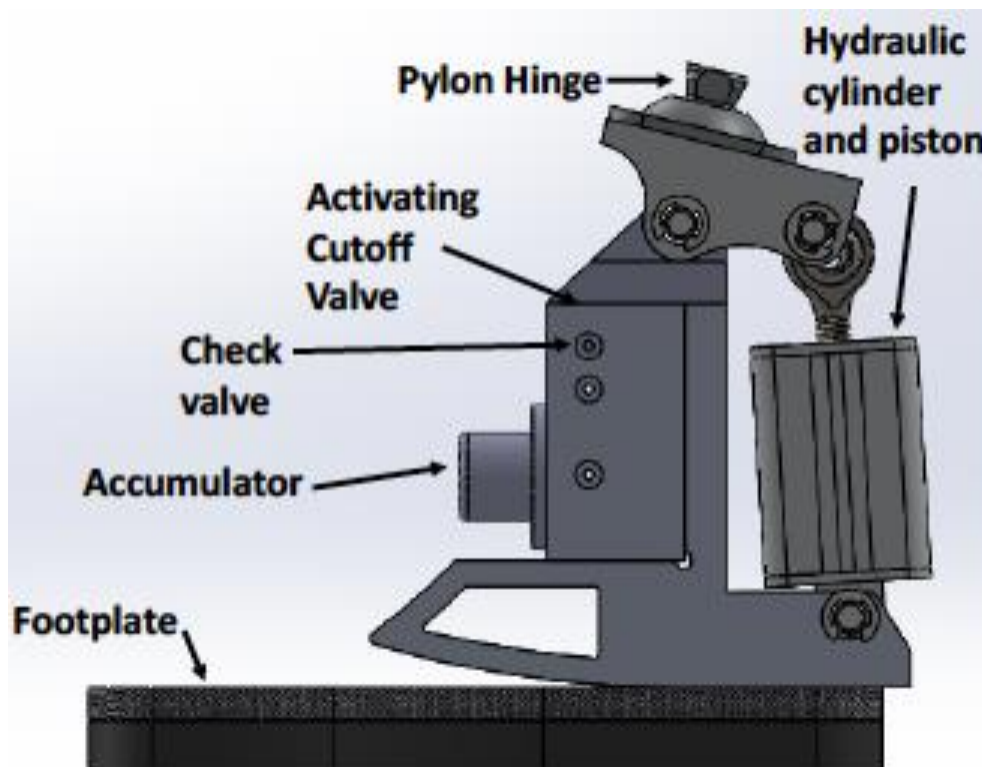
Figure 9. Amiot Et Al.'S Ankle Design (Amiot, et al. 2017)
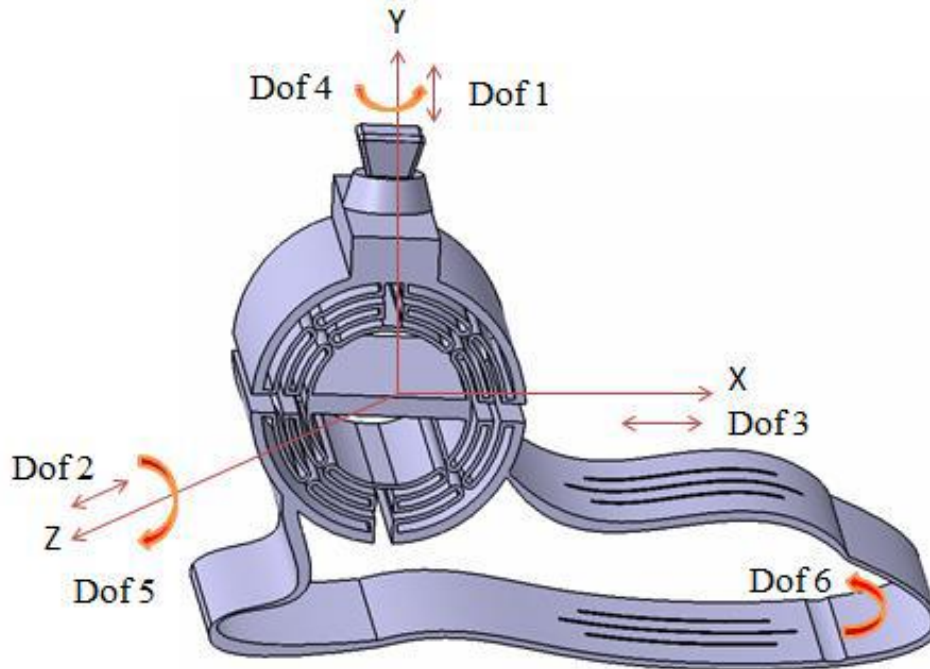
Figure 10. 6 DOF Compliant Ankle (Nguyen, Dao and Huang 2017)

1.4 Normal Human Gait

A normal gait varies from person to person. But every normal gait has the same cycle and phases. Figure 11 shows the various phases of a gait cycle of the right leg. The cycle starts with a heel strike followed by the flat foot stance and then toe-off. These three are a part of the stance phase. The swing phase follows the stance phase. During the swing phase, there is no ground reaction force acting on the foot. Hence, the swing phase acts as the transition between two consequent foot strikes.

Figure 12 shows a comparison between the ankle angle, moment, and power of the SACH foot and a healthy human ankle. It can be observed that the power transferred by the ankle spikes just before toe-off. This spike in power is difficult to obtain in a prosthetic ankle due to the peculiar nature of force delivered by the human leg muscles. This leads to the problem faced while designing a passive prosthesis. The proper problem statement or this thesis is discussed below.
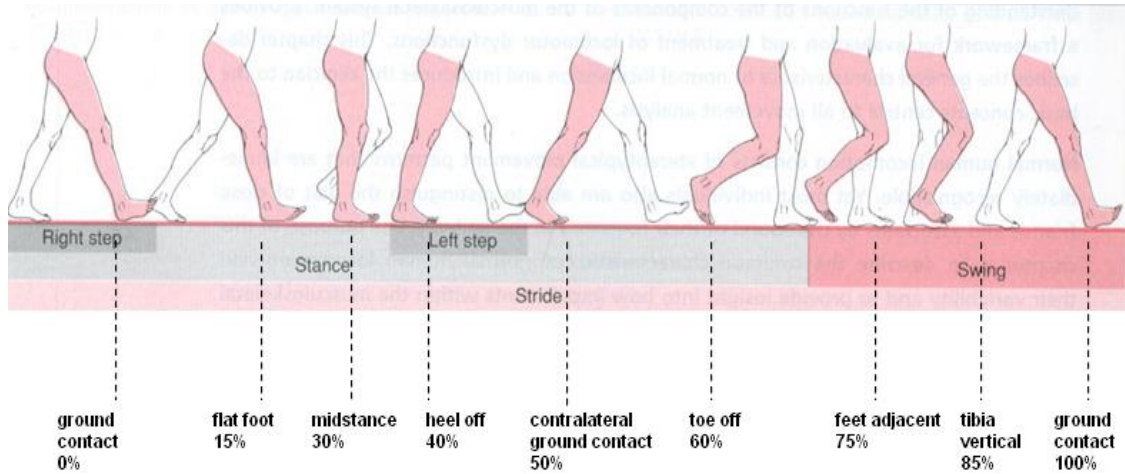
Figure 11. Phase of Gait Cycle of Right Leg (Hitt 2008)

1.5 Problem Statement

There is need for a prosthetic ankle which would give near normal gait with close to no power requirement while being relatively cheap. A passive prosthetic ankle requires no external power source and if properly tuned and designed, would be a better choice. The goal of this research is to design and develop a passive prosthetic ankle that gives ankle angle, moment, and power profiles close to that in Figure 12.

All the information studied above is applied to design and develop a passive prosthetic ankle. The next chapter explains the motivation and reasons behind the design of the proposed prosthetic device.
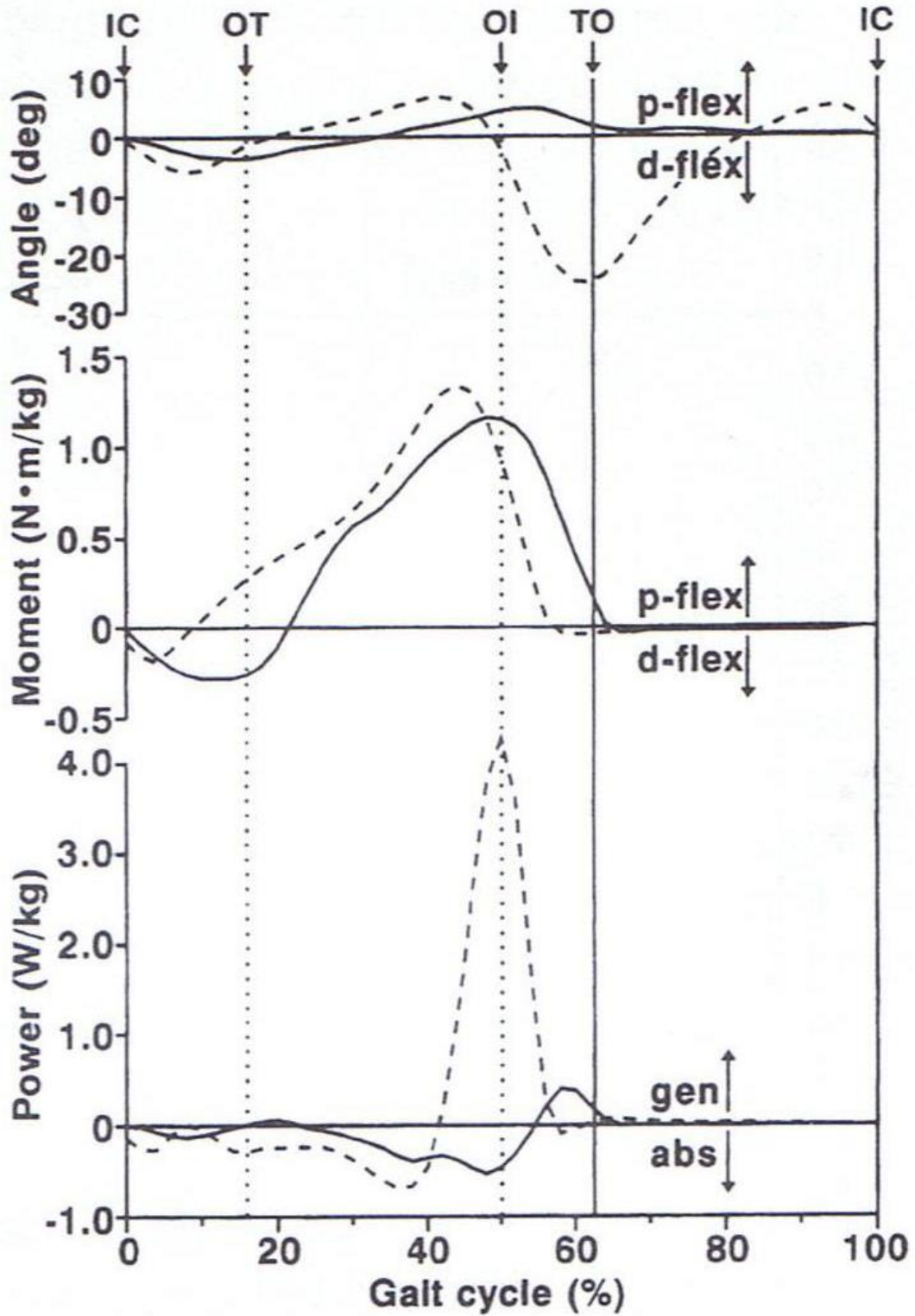
Figure 12. Comparison Between Ankle Angle, Moment, And Power of SACH Foot (Solid Line) Vs A Healthy Human Ankle (Dashed Line) (Hitt 2008)

CHAPTER 2

DESIGN & MANUFACTURING

The passive prosthetic ankle proposed here has a simple design which is inspired by the human ankle and the way tendons are aligned with respect to the bones. If human gait is observed as a single axis motion, two muscle groups and tendons play a very important role in absorbing the impact of heel strike and providing force during toe-off. These groups are the 'Gastrocnemius muscle' group along with the 'Achilles tendon' and the 'Anterior Tibial' muscle group and tendon. During heel strike, the Gastrocnemius muscles sustain the impact. Their main function is to plantarflex the foot. Dorsiflexion of the foot is attained primarily by the tibialis anterior muscle which aides in the toe-off phase. Other muscles in the group provide secondary dorsiflexion and are weak (Whittle 2007). All these muscle groups can be observed in Figure 13 (Whittle 2007).The orientation and location of these muscle groups has heavily influenced the design of the ankle. The ankle is also designed considering the human ankle's skeletal structure. The bones in the human foot can be seen in Figure 14.

To identify the angle and position of the muscle groups, some other research works were also studied. As evident from the work of P. Procter et al, the Achilles tendon is connected to the calcaneus at an angle of 87 degrees and the anterior tibial tendon is connected to the tarsal bones at an angle of 36 degrees (both in neutral pose) (P.Procter and J.P.Paul 1982). These angles change to 78 degrees and 38 degrees respectively during dorsiflexion and 98 degrees and 34 degrees respectively during plantarflexion (P.Procter and J.P.Paul 1982).

Patellar tendon

Peroneus longus

Tibialis anterior

Extensor digitorum longus

Peroneus brevis

Extensor hallucis longus

Gastrocnemius

Soleus

Gastrocnemius

Soleus

Achilles tendon
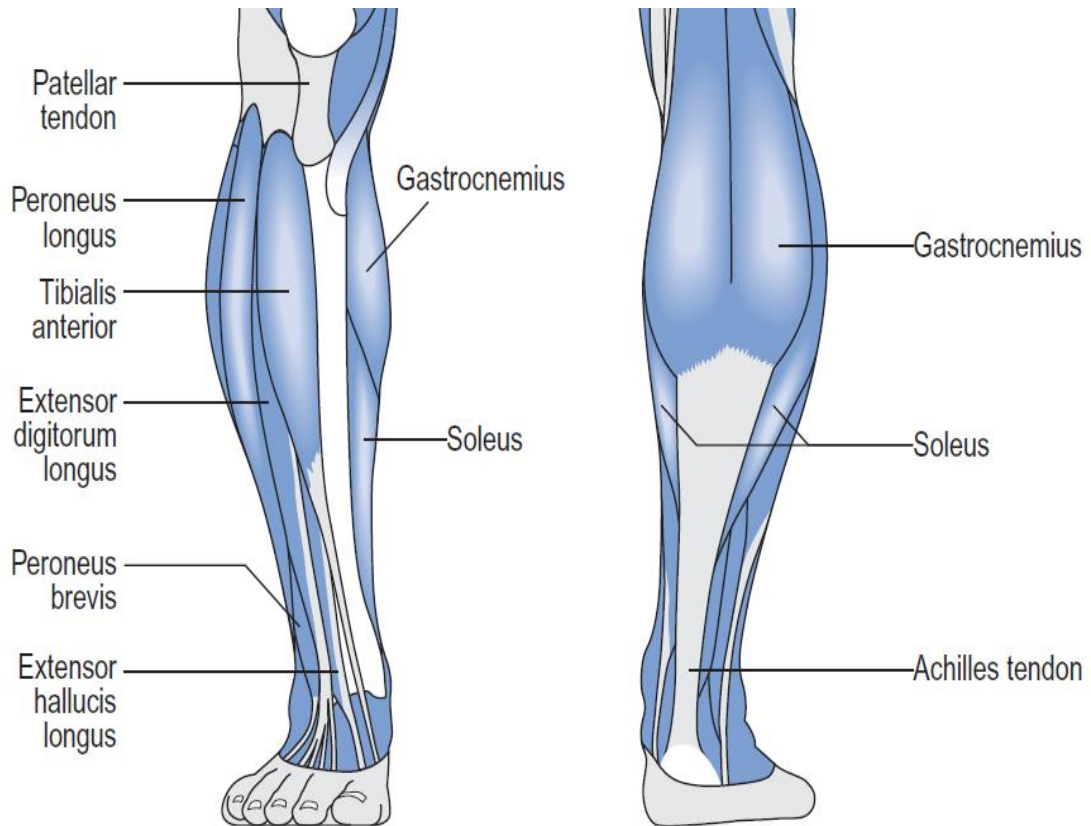
Figure 13. Muscle Structure of a Human Right Leg. (Whittle 2007)

Navicular

Medial cuneiform

Tibia

Talus

Calcaneus

Phalanges

First metatarsal
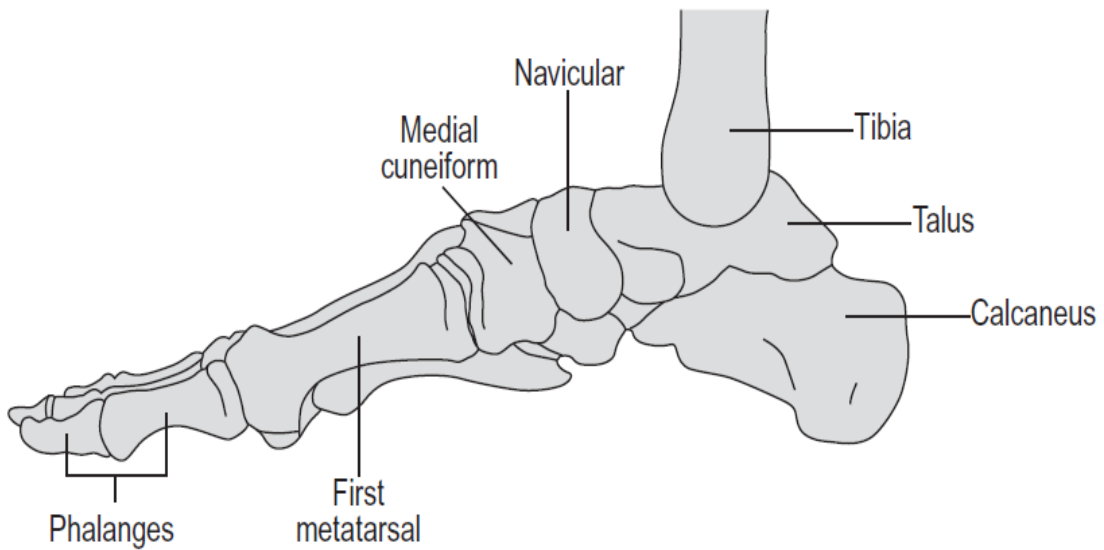
Figure 14. Skeletal Structure of Human Right Leg. (Whittle 2007)

15
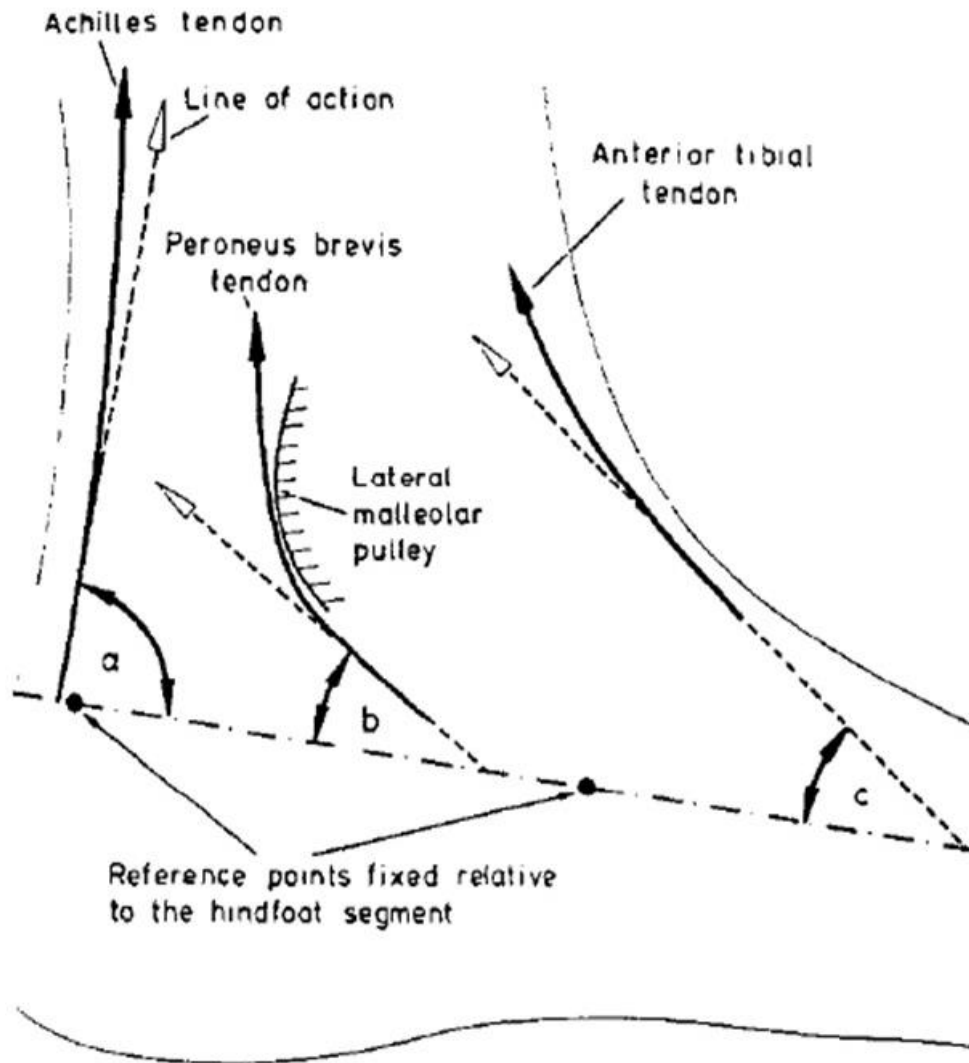
Figure 15. Angle Between Tendons and The Bones in A Human Foot. (P.Procter and J.P.Paul 1982)

The things discussed above inspired the design of the prosthesis. The design of the prosthetic ankle explained in the next section.

2.1 Design

After considering the above facts about the human ankle, it was decided that two springs are needed to control foot. Therefore, the ankle has two springs: one connected to the heel emulating the Achilles tendon and the second in the front emulating the Tibialis Anterior tendon. The design of the ankle is as shown in Figure 16.
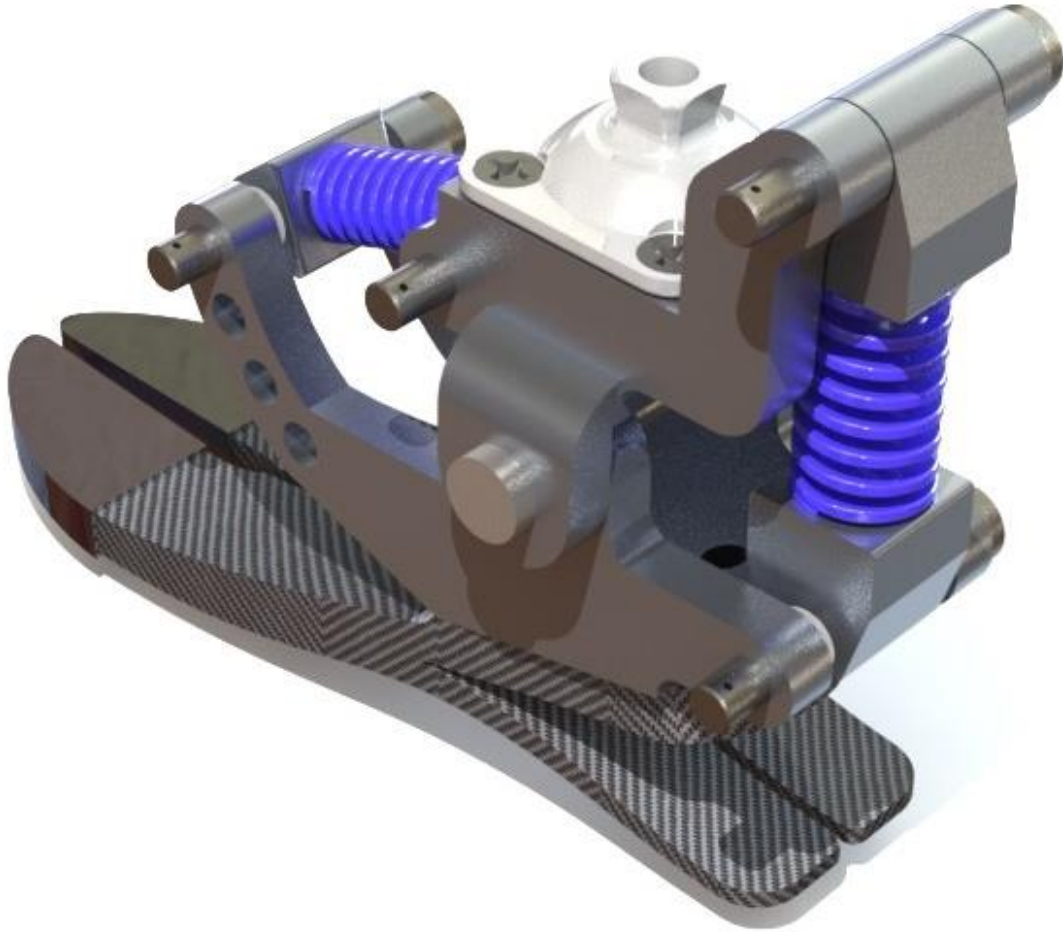
Figure 16. Final Design of The Passive Prosthetic Ankle

There are four parts in the ankle that were manufactured, the other parts were selected. The selected components are as follows. The ankle is mounted to the leg stump with a standard mounting pyramid. The prosthetic device's base is a carbon fiber foot which was selected because of its durability, flexibility, and low weight. A double shielded, single row, radial ball bearing sits on the pin connected to the part B. Each spring mount has a sleeve bearing connecting it to the pins. The springs were selected for their long life and high durability. The spring was selected based on the dynamics in section 2.3.
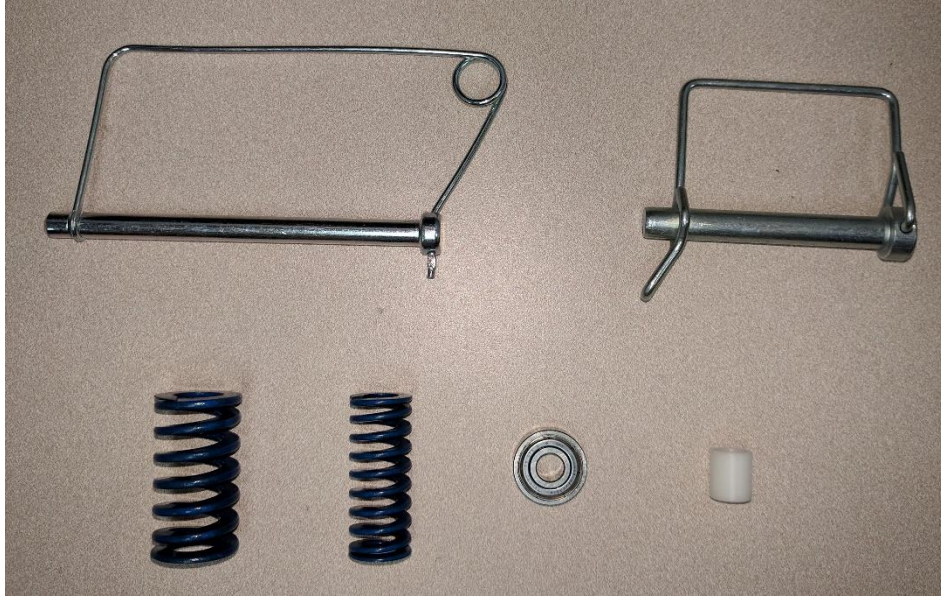
Figure 17. Top-Left to Right: Hinge-Pin, Spring Mount Pin, Heel Spring, Anterior Spring, Hinge Bearing, Spring Mount Sleeve Bearing
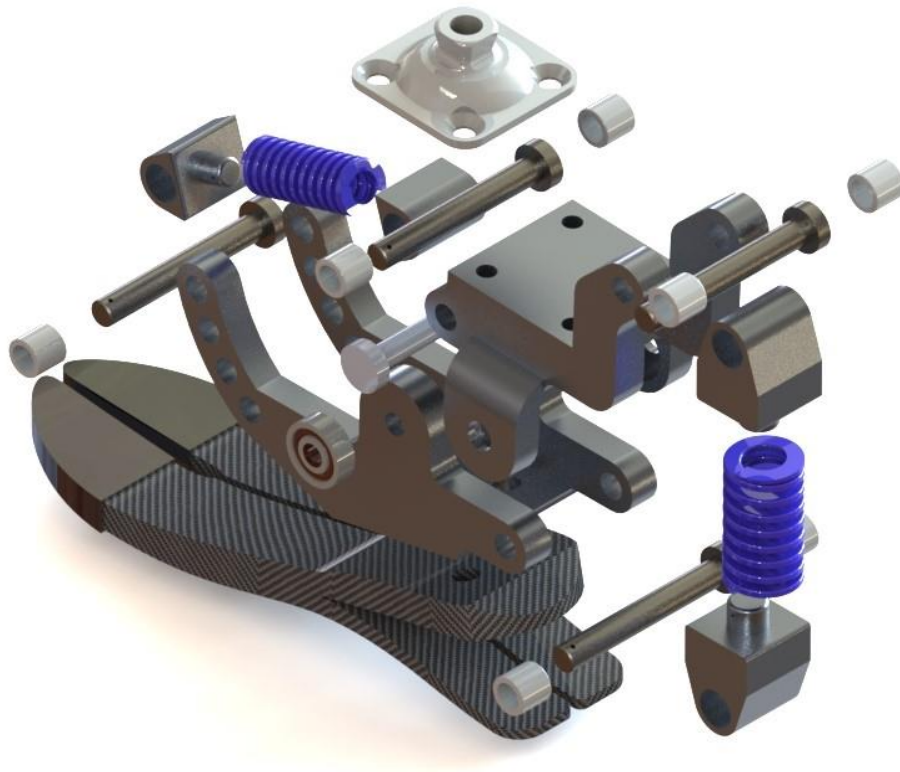
Figure 18. Exploded View of The Passive Prosthetic Ankle (Jaipurfoot.org 2016)

The above parts were carefully selected to ensure long life and durability. The manufactured parts were designed with similar intentions. The manufactured parts in the prosthetic ankle were as follows: part A, part B, heel spring mount, and the anterior spring mount. All the parts were designed to be manufactured out of Aluminum 6061-T6, which was selected for its high tensile strength, easy machinability, and cost efficiency. Table 1 shows the bill of material for the prosthetic ankle.

Table 1. Bill of Material

Sr. No.	Part Name	Material	Quantity
1.	Part A	AL 6061-T6	1
2.	Part B	AL 6061-T6	1
3.	Bearing 1	(multiple)	2
4.	Bearing 2	(multiple)	8
5.	Anterior spring mount	AL 6061-T6	2
6.	Heel spring mount	AL 6061-T6	2
7.	Freedom foot	Carbon fiber	1
8.	Pin 1	Steel	1
9.	Pin2	Steel	4

So far, the design aspects of the prosthetic ankle were discussed. It is now important to understand the method of operation of the passive prosthetic ankle. The next section elaborates the various phases of gait the prosthetic ankle undergoes followed by the dynamics of the system.

2.2 Method of Operation

To understand the phases of operation of the passive prosthetic ankle, the phases in human gait were projected onto the simulated prosthetic ankle. Figure 19 shows the various phases of gait cycle the passive prosthetic ankle might undergo. At heel-strike, the normal reaction force along with the friction force acts on the heel. This along with the weight of the amputee pushes the heel spring into compression and the anterior springs into extension. As the gait continues, the heel and anterior springs along with the force due to weight of the amputee provide the ankle with momentum to push the ankle into the flat foot position. The same momentum takes the ankle into mid-stance where the heel spring is elongated, and the anterior spring is compressed. Next comes the heel-off phase where the ankle starts providing a forward thrust to the user. At toe-off, the compressed anterior spring provides the push needed to propel the amputee.

| 0% of gait cycle (heel-strike) | 5% of gait cycle | 15% of gait cycle (flat foot) |
| 30% of gait cycle (mid-stance) | 40% of gait cycle (heel-off) | 60% of gait cycle (toe-off) |
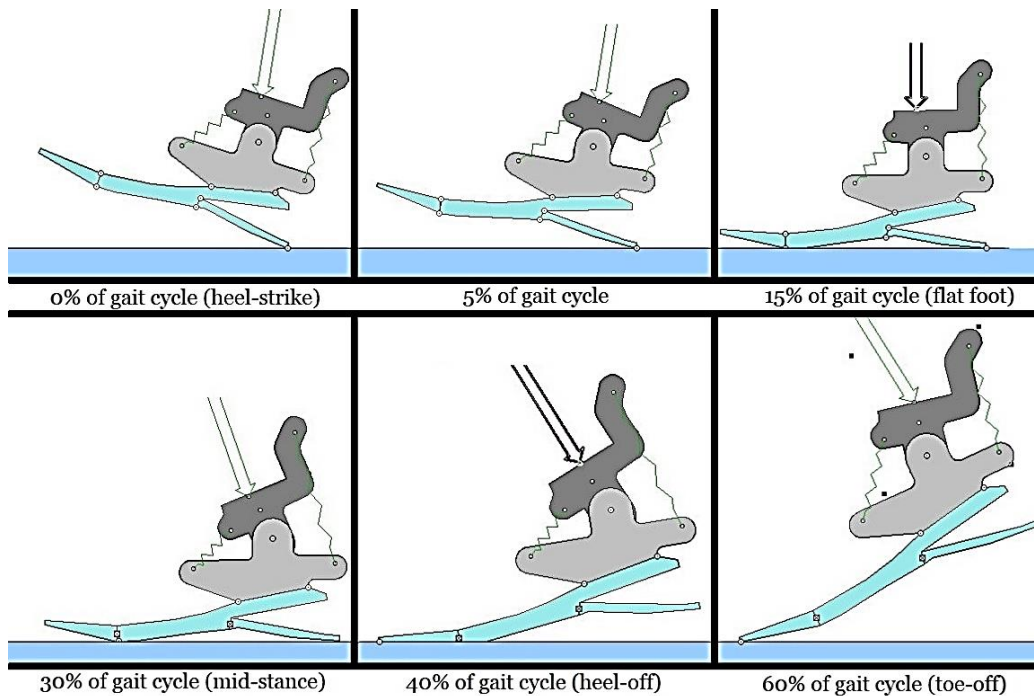
Figure 19. Gait Cycle for The Passive Prosthetic Ankle

A general idea of how the passive prosthetic ankle might operate was discussed above. It was necessary to formulate the dynamics of the ankle with respect to the ankle operation. Those equations were required to simulate the response of the ankle to external stimulus. The dynamics of the passive prosthetic ankle will be discussed in the next section.

2.3 Dynamics

Seeing how the dynamics of an ankle can be complicated, the prosthetic ankle is imagined as a simple two body, mass, and spring system. Figure 20 shows the spring mass system. The two bodies have masses 'm' and 'm1'. The neutral axis of the ankle can be imagined as an imaginary line passing through the ankle hinge perpendicular to the foot. There are three stages in the dynamics of the prosthetic ankle. The dynamic equations for all three stages are discussed below.
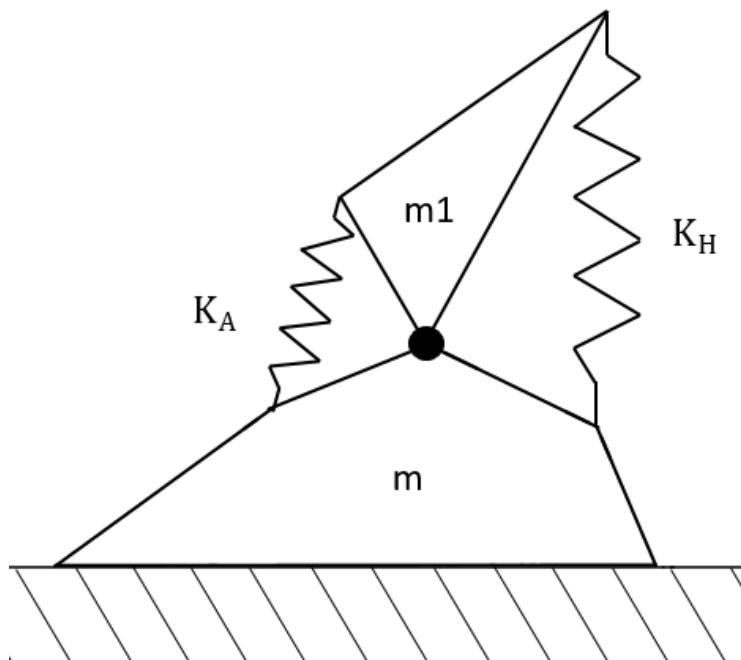
Figure 20. Spring Mass System Representing the Prosthetic Ankle

1. Heel-strike to flat-foot:
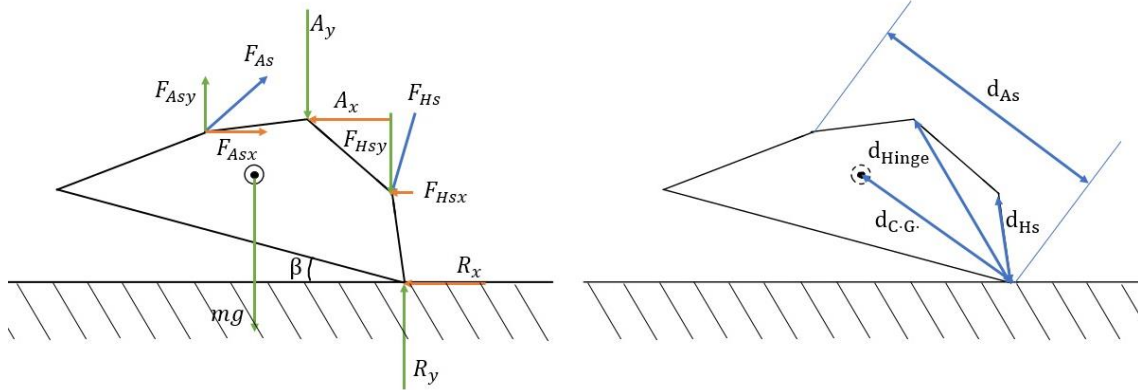
Figure 21. Free Body Diagram for Case 1 (Left); Distance Of Points From The Heel (Right)

Assuming there is no slip at the point of contact, and the angle the spring makes with the neutral axis doesn't change with the gait (the change is negligible and doesn't have a prominent effect on the dynamics of the prosthetic ankle) the dynamics equations were derived.

Figure 21 shows the free body diagram of the lower part of the ankle and the distances needed for the moment equation. The FBD will be used to formulate the dynamics equations. The following are the notations used in the dynamics equations:

a_x : acceleration of the foot in the x direction about the center of gravity

a_y : acceleration of the foot in the y direction about the center of gravity

R_x : x component of the Ground Reaction Force (GRF)

R_y : y component of the GRF

A_x : x component of the force acting on the ankle hinge

A_y : y component of the force acting on the ankle hinge

m : mass of the foot

F_{As} : force exerted by the anterior spring

F_{Hs} : force exerted by the heel spring

K_A : spring co-efficient of the anterior spring

K_H : spring co-efficient of the heel spring

Δl_{As} : deflection of the anterior spring

Δl_{Hs} : deflection of the heel spring

θ : relative angle between the neutral axis and the shank (zero when standing)

β : angle between the ground and the foot

Newton's second law of motion states:

$$\sum F = ma$$

The acceleration term is split into two components viz. a_x and a_y

$$\begin{bmatrix} \sum F_x \\ \sum F_y \end{bmatrix} = m \begin{bmatrix} a_x \\ a_y \end{bmatrix}$$

All the forces are substituted as seen in the Free Body Diagram in Figure 21.

$$m \begin{bmatrix} a_x \\ a_y \end{bmatrix} = \begin{bmatrix} F_{Asx}(\theta, \beta) - R_x - F_{Hsx}(\theta, \beta) - A_x \\ F_{Asy}(\theta, \beta) + R_y - F_{Hsy}(\theta, \beta) - A_y - mg \end{bmatrix}$$

$$m \begin{bmatrix} a_x \\ a_y \end{bmatrix} = \begin{bmatrix} K_A \Delta l_{As}(\theta)\cos(54 + \beta) - R_x - K_H \Delta l_{Hs}(\theta)\sin\beta - A_x \\ K_A \Delta l_{As}(\theta)\sin(54 + \beta) + R_y - K_H \Delta l_{Hs}(\theta)\cos\beta - A_y - mg \end{bmatrix} \quad (2.1)$$

Now, the moment is calculated about the heel C.G:

$$\sum M = I\alpha$$

$$I\alpha = mg \times d_{C \cdot G.} - F_{As} \times d_{As} + F_{Hs} \times d_{Hs} + A \times d_{Hinge} \quad (2.2)$$

The symbol '×' denotes a cross product of the two entities.

23

2. Flat-foot:

The second stage in the dynamics is the flat foot phase shown in Figure 22.. The dynamics equations are as given below.
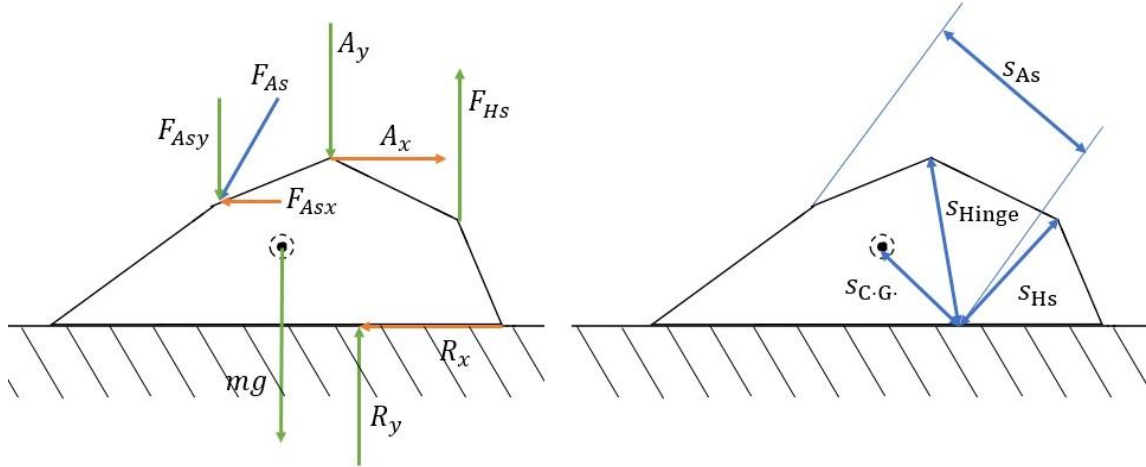
Figure 22. Free Body Diagram for Case 2 (Left); Distance Of Points From The Center Of Pressure Of Ground Reaction Force (Right)

Applying newton's second law,

$$\sum F = ma$$

$$\begin{bmatrix} \sum F_x \\ \sum F_y \end{bmatrix} = m \begin{bmatrix} a_x \\ a_y \end{bmatrix}$$

$$m \begin{bmatrix} a_x \\ a_y \end{bmatrix} = \begin{bmatrix} A_x - F_{Asx}(\theta) - R_x \\ R_y - F_{Asy}(\theta) + F_{Hsy}(\theta) - A_y - mg \end{bmatrix}$$

$$m \begin{bmatrix} a_x \\ a_y \end{bmatrix} = \begin{bmatrix} A_x - K_A \Delta l_{As}(\theta) \cos(54) - R_x \\ R_y - K_A \Delta l_{As}(\theta) \sin(54) + K_H \Delta l_{Hs}(\theta) - A_y - mg \end{bmatrix} \qquad (2.3)$$

Now, the moment is calculated about the center of pressure of the ground reaction force:

$$\sum M = I\alpha$$

$$I\alpha = mg \times s_{C.G.} + F_{As} \times s_{As} + F_{Hs} \times s_{Hs} + A \times s_{Hinge} \qquad (2.4)$$

24

3. Flat-foot to toe-off:

Toe-off follows flat foot is a typical gait. The dynamics for this stage are formulated below using Figure 23.
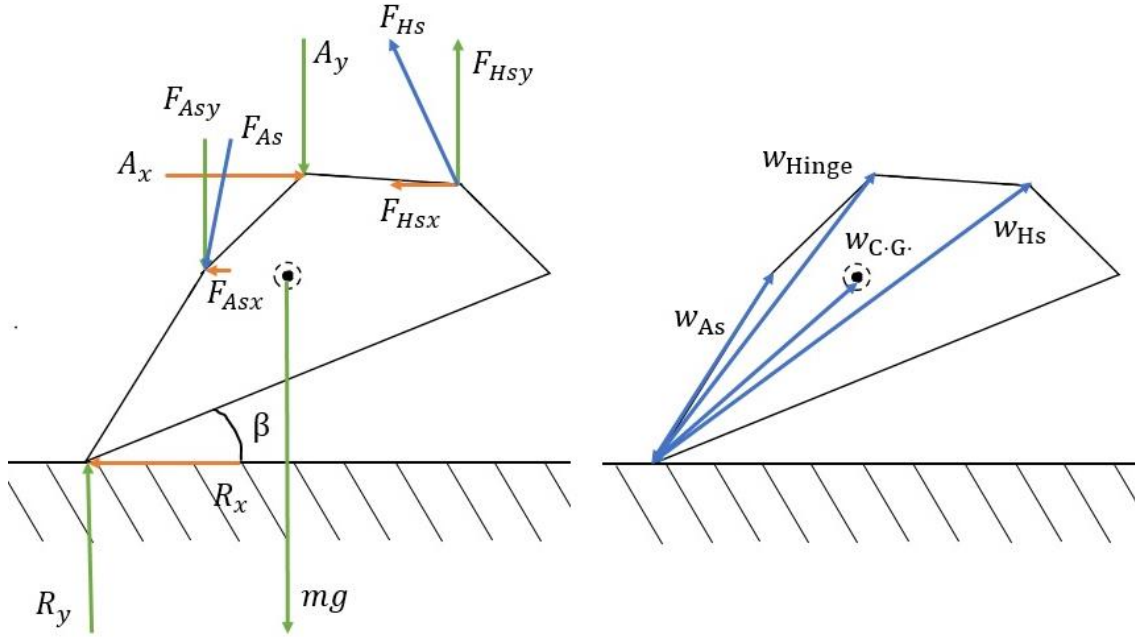
Figure 23. Free Body Diagram for Case 3 (Left); Distance Of Points From The Toe (Right)

Applying newton's second law,

$$\sum F = ma$$

$$\begin{bmatrix} \sum F_x \\ \sum F_y \end{bmatrix} = m \begin{bmatrix} a_x \\ a_y \end{bmatrix}$$

$$m \begin{bmatrix} a_x \\ a_y \end{bmatrix} = \begin{bmatrix} A_x - F_{Asx}(\theta, \beta) - R_x - F_{Hsx}(\theta, \beta) \\ R_y - F_{Asy}(\theta, \beta) + F_{Hsy}(\theta, \beta) - A_y - mg \end{bmatrix}$$

$$m \begin{bmatrix} a_x \\ a_y \end{bmatrix} = \begin{bmatrix} A_x - K_A \Delta l_{As}(\theta) \cos(54 + \beta) - R_x - K_H \Delta l_{Hs}(\theta) \sin \beta \\ R_y - K_A \Delta l_{As}(\theta) \sin(54 + \beta) + K_H \Delta l_{Hs}(\theta) \cos \beta - A_y - mg \end{bmatrix} \quad (2.5)$$

Now, the moment is calculated about the toe:

$$\sum M = I\alpha$$

$$I\alpha = F_{As} \times w_{As} - mg \times w_{C \cdot G \cdot} - F_{Hs} \times w_{Hs} - A \times w_{Hinge} \quad (2.6)$$

25

The equations 2.1, 2.3, and 2.5 relate a_x and a_y to θ and β. The equations contain many

unknown variables that change based on the propagation of the gait. The system is

quite complicated to solve in the closed form. Thus, a simulation software (working

model 2D) was used to solve the dynamics. The simulation operated in the discrete

time domain. Torque was calculated by the software and put through post processing.
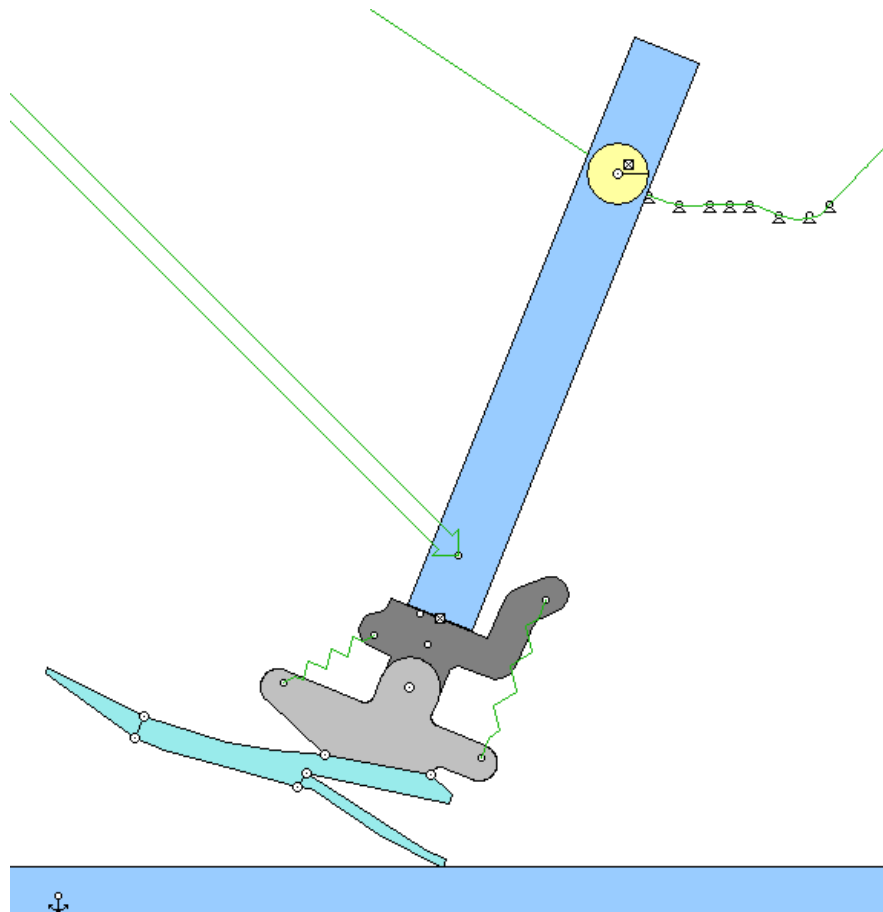
Figure 24. Working Model 2D Simulated Ankle

Figure 24. Working Model 2D Simulated Ankle shows the model used for simulation.

All the parts were given their respective mechanical properties viz. friction coefficient,

mass, etc. The shank on top of the ankle was given some weight to simulate a healthy

human body. A force was applied at the shank to help the simulated leg perform gait.

The trajectory of the simulated knee was obtained from an article by Varela et al.

(Varela, Ceccarelli and Flores 2015). Varela and his team performed motion capture of a healthy human gait to obtain the trajectory in Figure 25
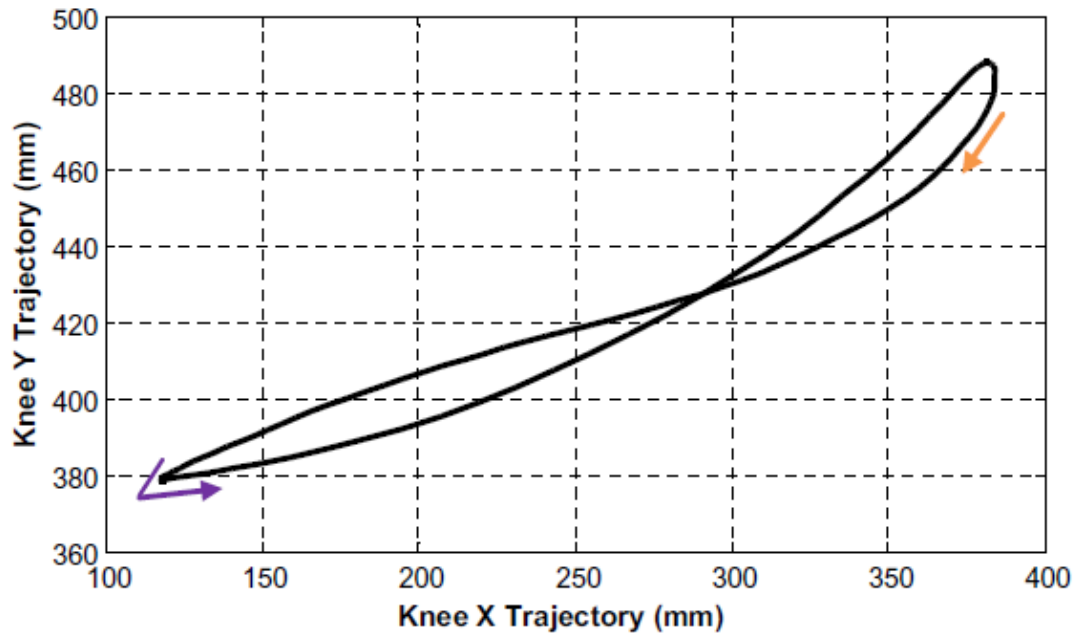
Figure 25. Knee Trajectory in The Sagittal Plane (Varela, Ceccarelli and Flores 2015)

Multiple combinations of anterior and heel spring stiffness were used to get a spectrum of data for comparison. Figure 26 shows the data collected from the simulation. The control data was that of a healthy human ankle taken from the information in Figure 12. H6A4 meant that the Heel spring to Anterior spring ratio was close to 6:4 and so on with the others. The data showed a Heel spring to Anterior spring ratio of 5:3 was optimum out of the compared data as the moment spikes were closer to the control data.

It was difficult for the simulation to calculate the data associated to the ankle dynamics due to the inaccuracies in the model creation and the difference between a simulated gait and a real gait. The data was then verified via multiple experiments as discussed in Chapter 3.
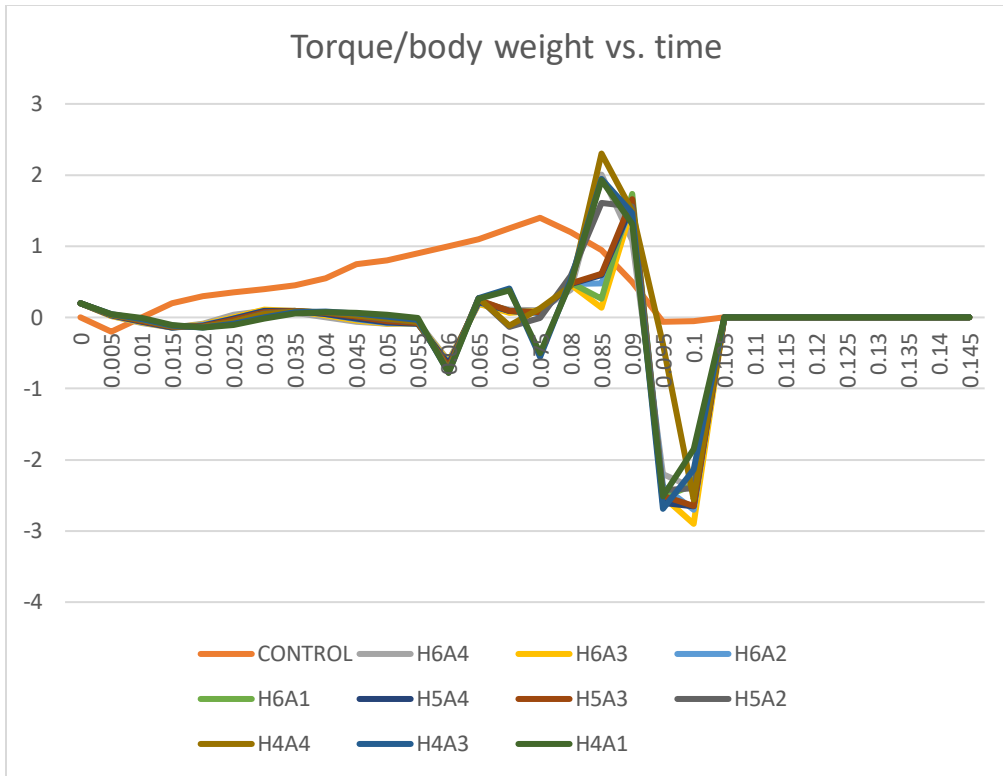
Figure 26. Comparison of Torque Data
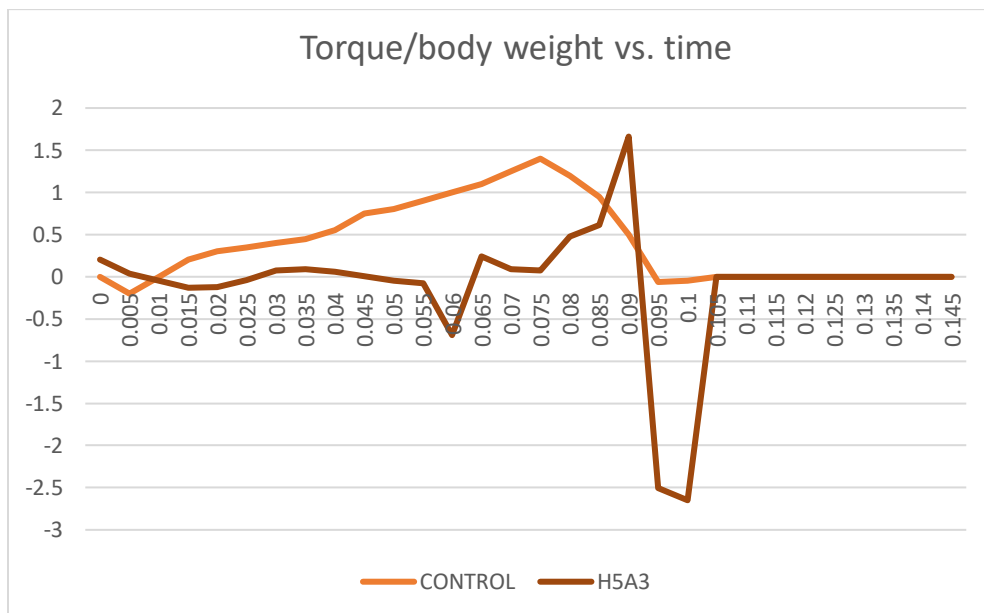
Figure 27. Torque/ Body Weight Vs. Time for The Simulated Prosthetic Ankle

After selecting the springs, the designed parts were tested for stress failure. A finite element method was used to check the stress concentration in the design under specific loading situations. The next section describes the results of the finite element analysis

2.4 Finite Element Analysis

All the designed parts were analyzed for loads with at least a factor of 2.5 to prevent failure. The results were as follows. Figure 28 shows the stresses on part A with forces due to the ankle hinge. The figure shows only a few red areas near the hinge pin hole. Figure 29 shows the stresses on part A with forces due to the heel spring. There were some high stress areas near the fillet underneath the arm, but still the part is safe. Figure 30 shows part A being loaded due to the anterior spring. The stress was concentrated where the arm meets the body, which can lead to deformation under higher loads. But for the spring selected, the design was safe. Figure 31 shows the stress due to the anterior spring on part B. The stress was not concentrated in any region as no red areas can be seen. Figure 32 shows the effect of the heel spring forces on part B. The stress was high in the hinge area, close to the yield strength of Aluminum 6061-T6 but because of the factor of safety, the design was safe. Figure 33 shows part B loaded due to the body weight of the amputee. The part was deformed on the top where the pyramid was going to be mounted. Figure 34 shows the heel spring mount being loaded by the spring under compression. The stress was highest on the seat. Figure 35 shows the anterior spring mount with a compressed anterior spring.

The analysis showed that the maximum stress acting on any of the parts was below the yield strength of Al 6061-T6. This meant the parts were safe to be tested in real life. In the next section, the ankle prototypes will be discussed.
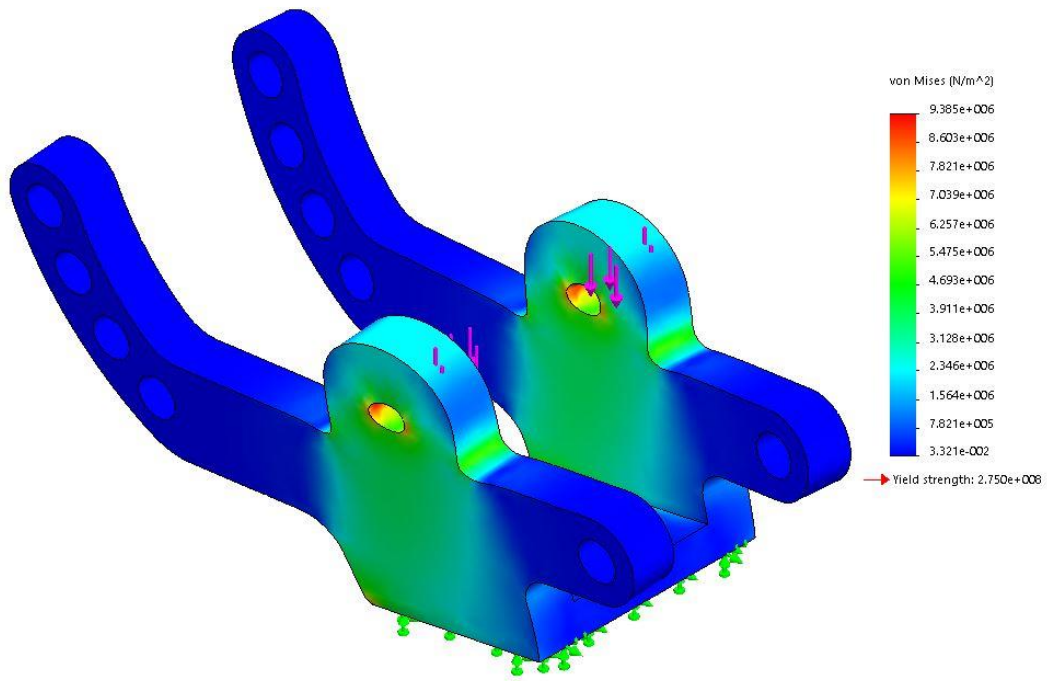
Figure 28. FEA of Ankle Part-A with Forces Due to Ankle Hinge
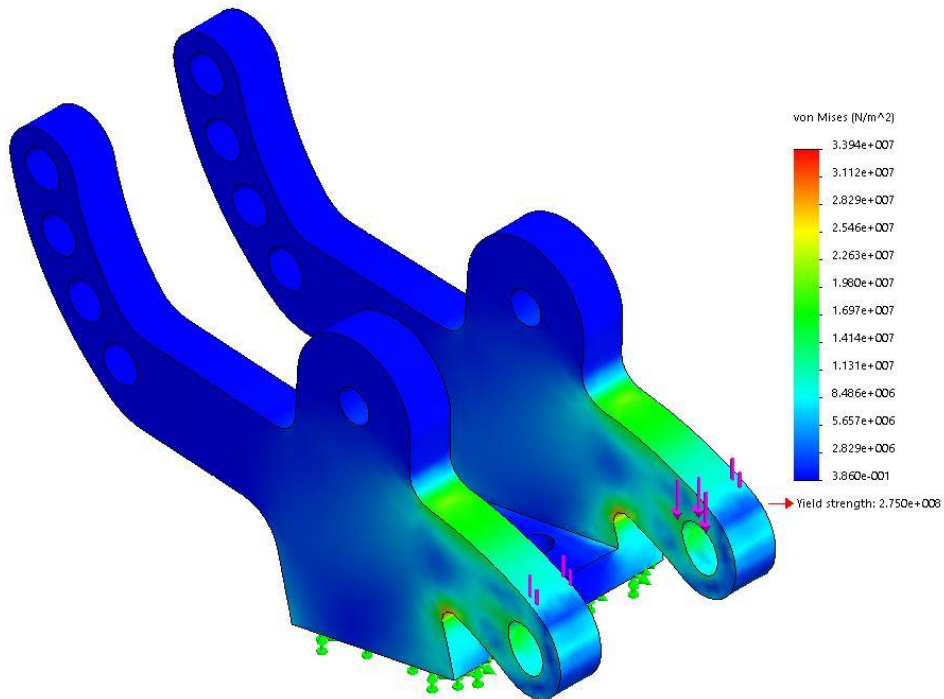
Figure 29. FEA of Ankle Part-A with Forces Due to Heel Spring

30
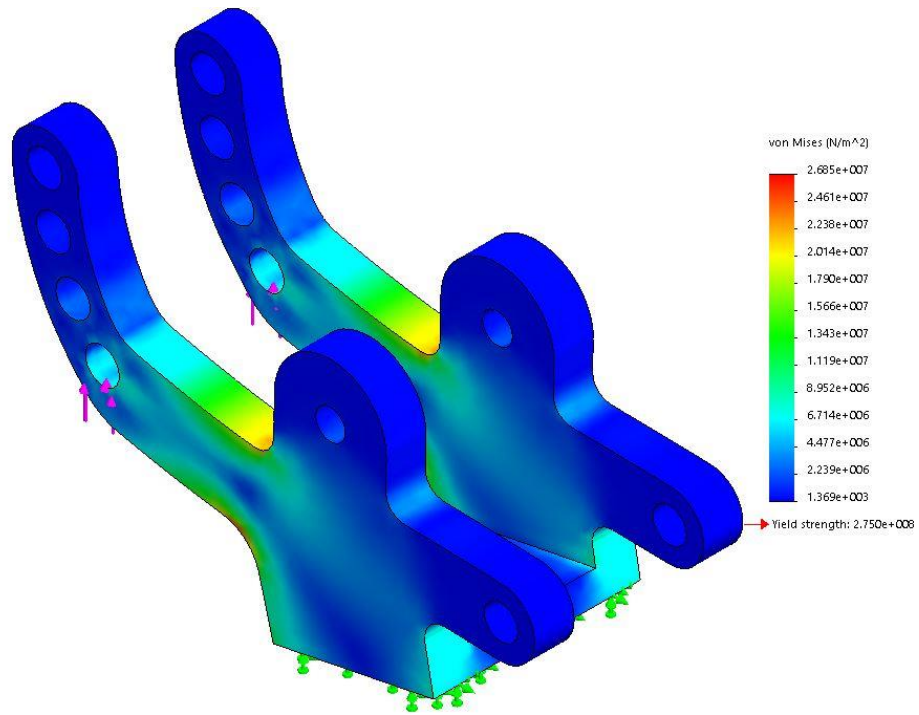
Figure 30. FEA of Ankle Part-A with Forces Due to Anterior Spring
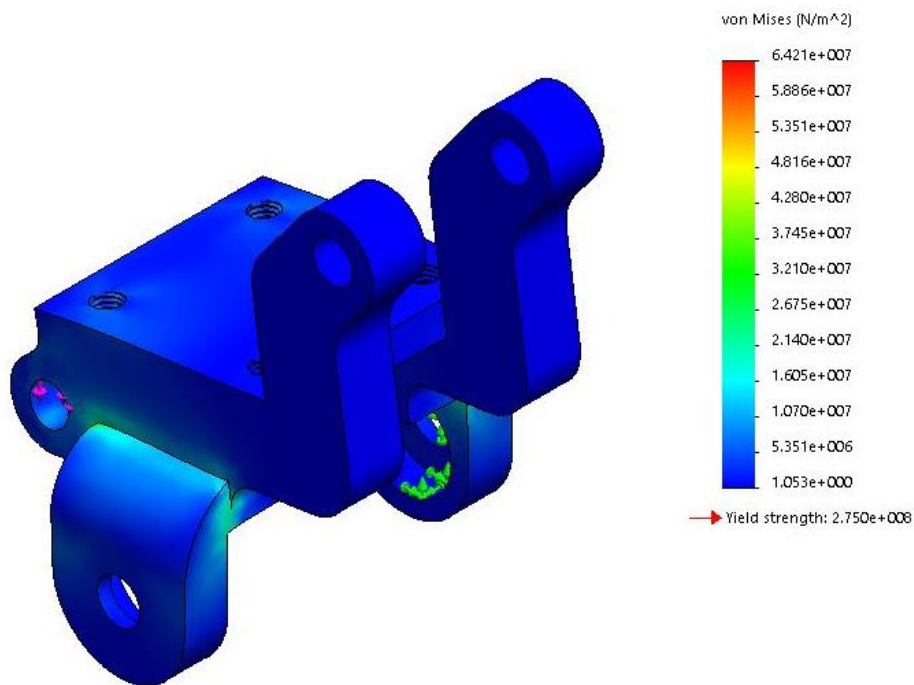
Figure 31. FEA of Ankle Part-B with Forces Due to Anterior Spring
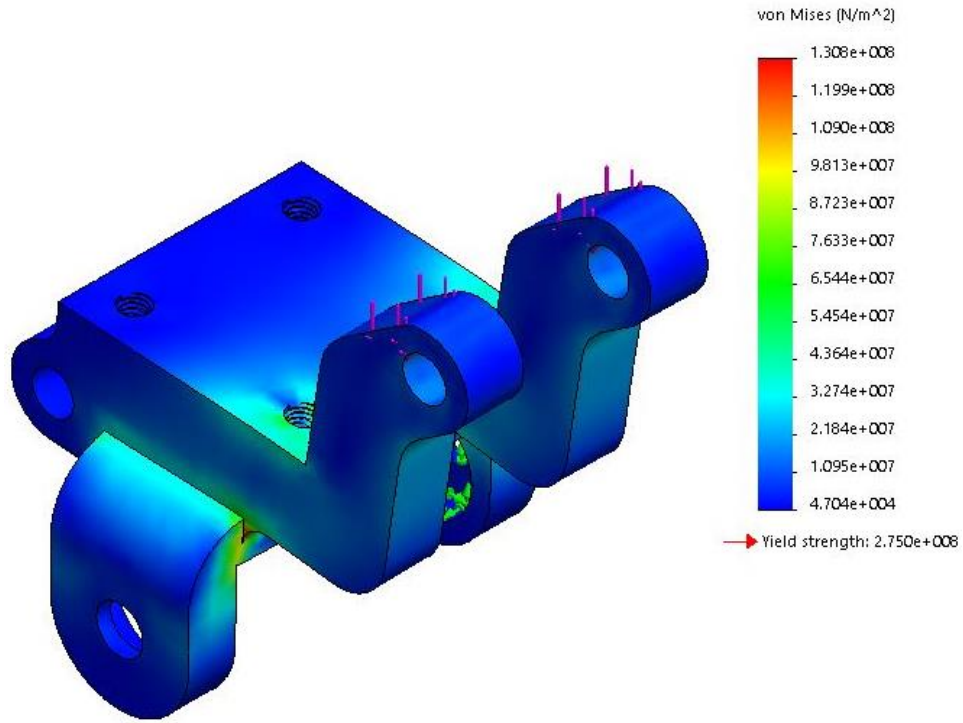
Figure 32. FEA Of Ankle Part-B with Forces Due to Heel Spring
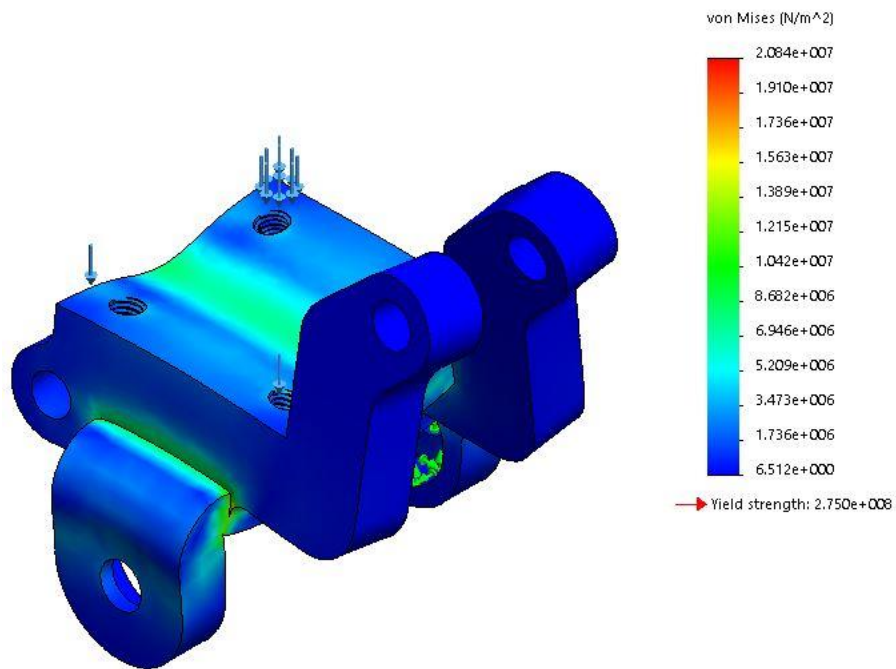
Figure 33. FEA of Ankle Part-B with Forces Due to Connecting Pyramid
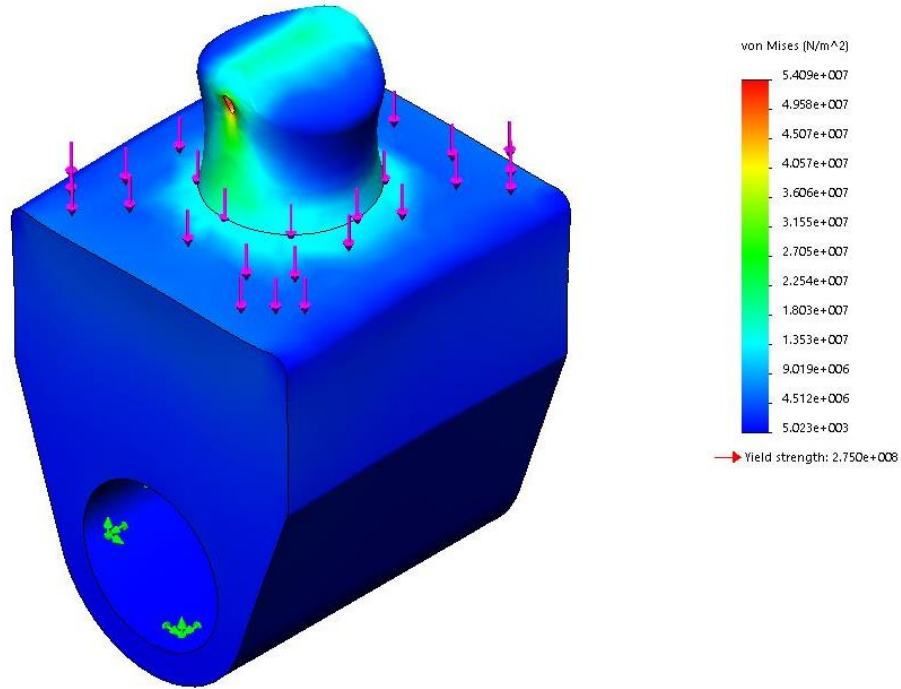
Figure 34. FEA of Heel Spring Mount During Spring Compression
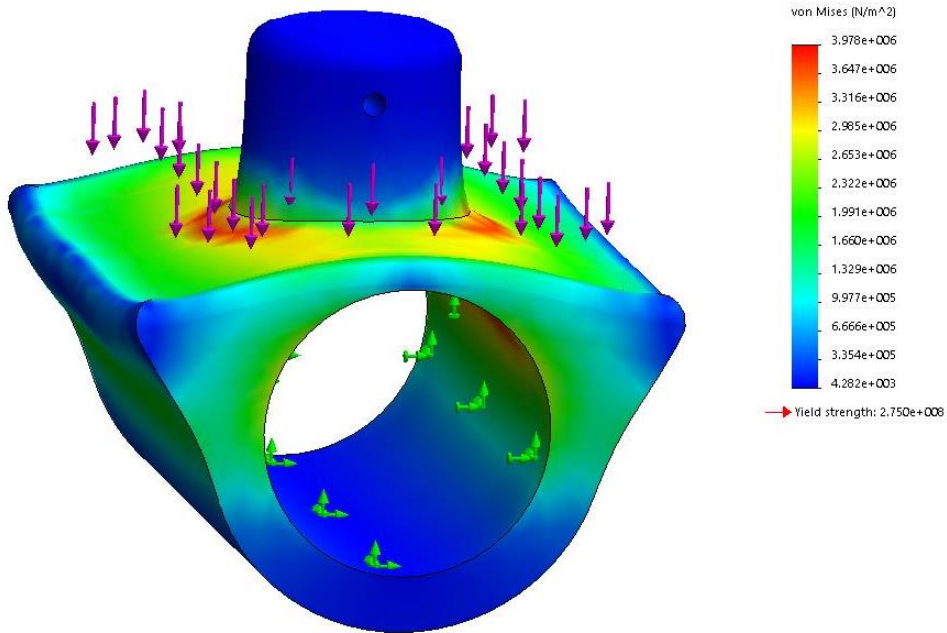
Figure 35. FEA of Anterior Spring Mount During Spring Compression
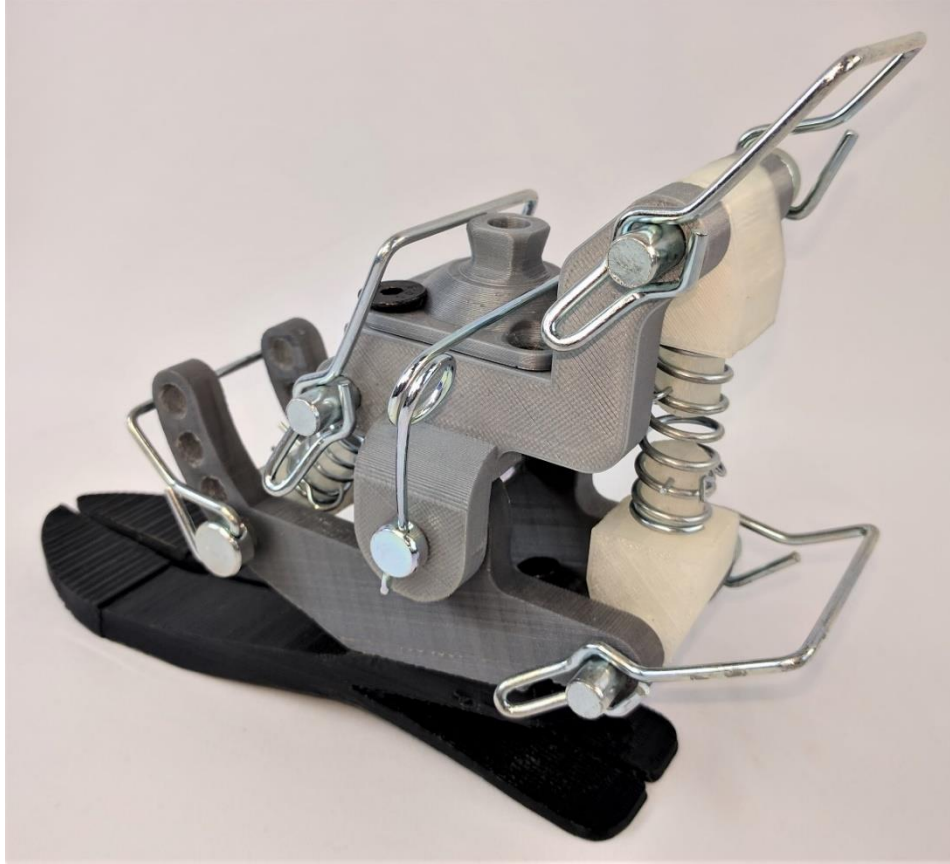
Figure 36. 3D Printed Passive Prosthetic Ankle.

2.5 Prototypes

To test the ankle design for any mechanical failures, an ankle was 3D printed to test on lower loads than the actual design. These 3D printed prototypes were used in various experiments discussed in Chapter 3. Figure 36 shows one of the prototypes printed for experimentation purpose.

The design and manufacturing of the passive prosthetic ankle was discussed in this chapter. With the above design and prototypes, some experiments were conducted to verify the results of the simulation. These experiments will be explained in the next chapter.

CHAPTER 3

EXPERIMENTATION

To authenticate the simulation data, to verify the actual usage of the prosthetic ankle, and to check the level of exertion while donning the device, the ankle prototype was tested two different ways. First a preliminary test was conducted to check whether the ankle supported the user like a real ankle. Upon getting affirmative results, the second, detailed experiment was conducted. In the next section, the pilot experiment will be discussed along with the results.

3.1 Preliminary Test

3.1.1. Aim

The objective of the test was to compare the ground reaction forces (GRF) generated by the prosthetic ankle to that of the human ankle. The experiment demanded accurate gait execution with lower loads because of the material used in the 3D printed ankle.

3.1.2. Apparatus and Preparation

To ensure proper gait and tunable load parameter, it was decided to use a robotic arm with approximately 20% the load on a human ankle which is averaged to be 80kg.

A Baxter collaborative robot was used to test the 20% force scale model. The 3D printed ankle was attached to the end effector of Baxter's left arm. Figure 37 shows the Baxter robot in its normal pose. A NeuLog NUL-225 force plate was used to measure the GRF on the ankle.
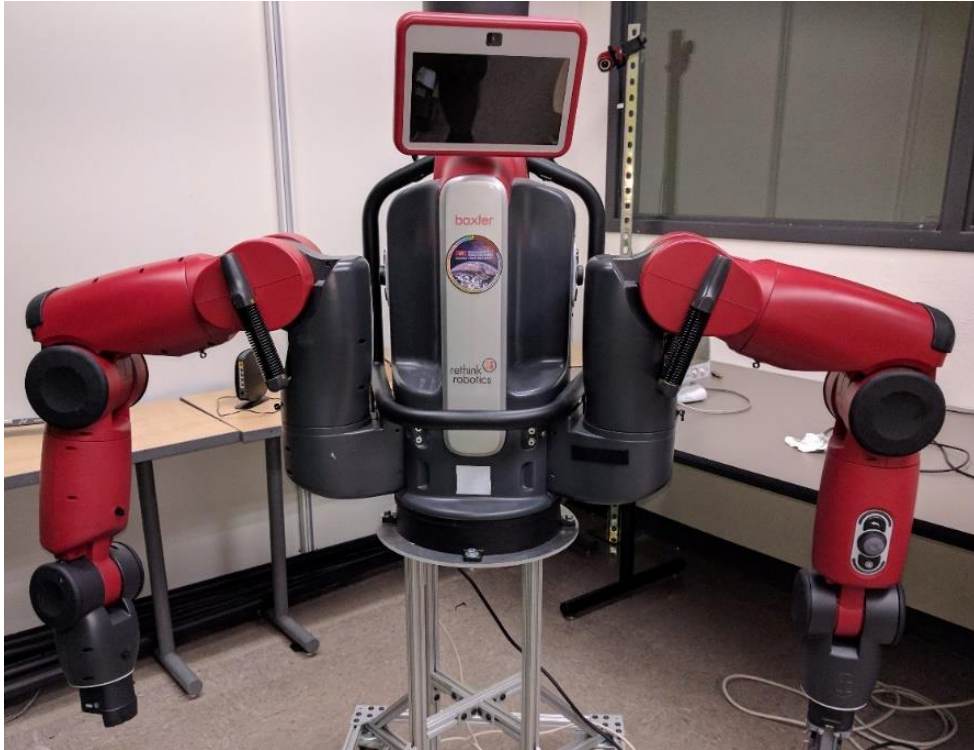
Figure 37. Baxter Collaborative Robot

Baxter robot is a collaborative industrial robot. Its purpose is basic tasks like pick and place, sorting, etc. It is also used for research in many universities (Baxter 2008). It operates on Robot Operating System (ROS) indigo version. All the joints are programmable through .rec files where every time stamp has an angle corresponding to every joint. For the experiment, the joints are programmed to mimic human gait. The elbow(E0) acts as the hip joint and the wrist(W1) acts as the knee joint with W0 at 90 degrees (Figure 38).

The prosthetic ankle was attached to Baxter's arm as shown in Figure 39 using a custom designed intermediate connector (Figure 40). The angles for the arm joints (knee and hip for the prosthetic ankle) were converted into the required format from the angles from Figure 12. The motion of the ankle was verified by visual inspection, and the experiment was conducted.
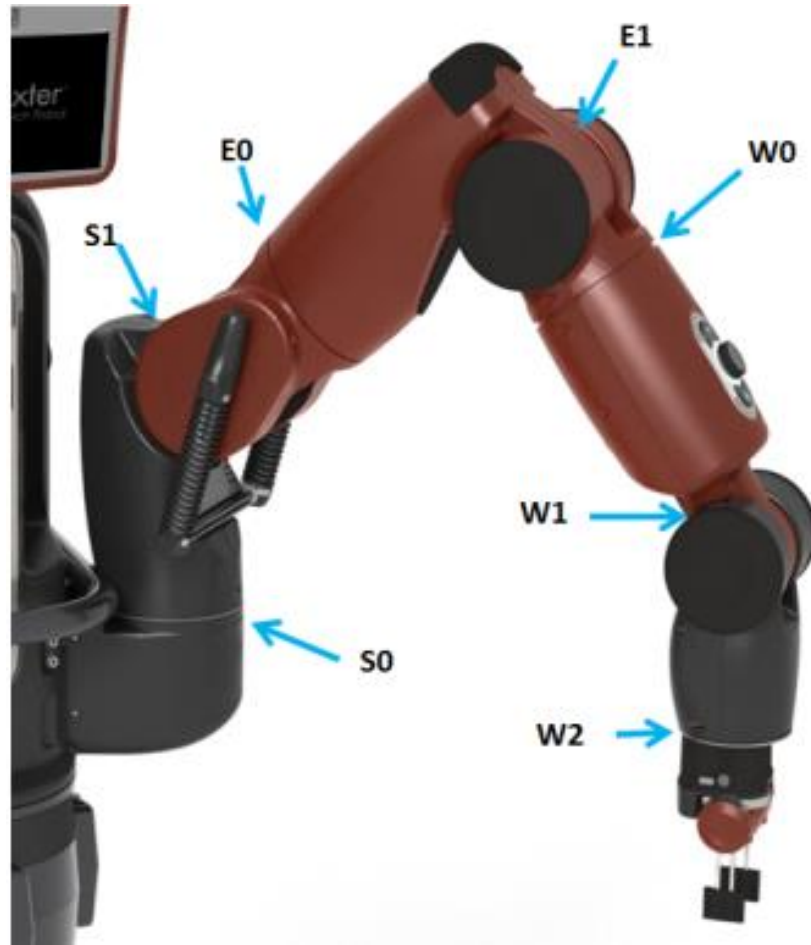
Figure 38. Baxter Arm with The Joints Labeled (Arms 2015)

3.1.3. Execution

The force plate measured forces in the vertical axis with no data on center of pressure. This warranted the need for a reference data set. Therefore, a human ankle's GRF was measured, averaged, and verified using the graph in Michael Whittle's book (Whittle 2007). Then, the prosthetic ankle was moved on the force plate by the robotic arm. The GRF data from the prosthetic ankle was collected for multiple runs and then averaged. Both the averaged data from the human ankle and the prosthetic ankle were plotted as in Figure 41. The profile of the GRF from the prosthetic ankle was compared to that of a healthy human ankle.

Figure 39. Prosthetic Ankle Attached to Left Arm Of Baxter
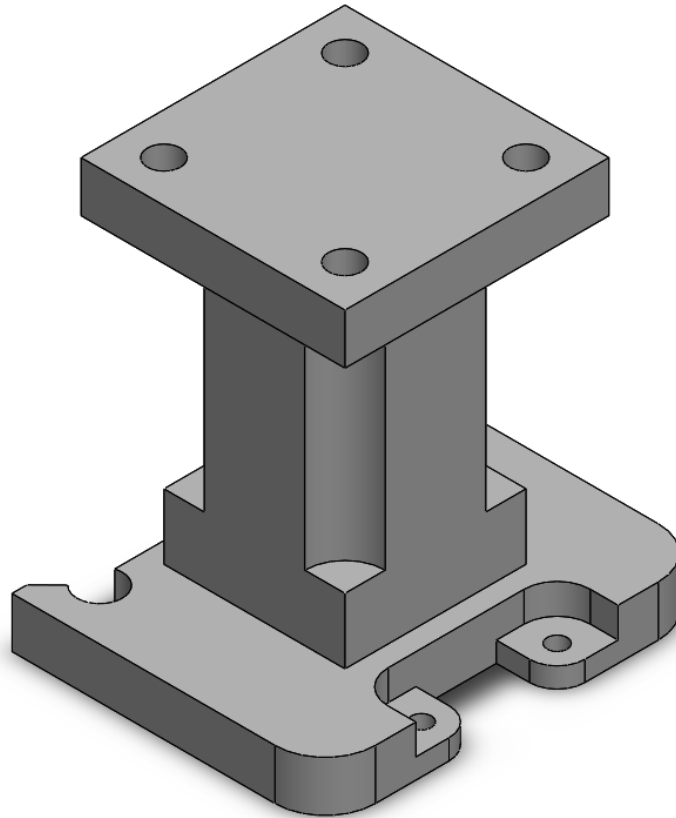
Figure 40. CAD Model of End Effector Connector

3.1.4. Results and Observations

The GRF for the human ankle formed a curve with two humps. The first hump occurs just after heel strike with the second one coming just before toe-off. The transitions are steep for GRF from the human ankle with the first hump narrower than the second hump. The GRF from the prosthetic ankle also form a two-humped curve with slightly different characteristics. The transition to the peak GRF is less steep signaling that the GRF rises sometime after the heel strike. The GRF remains at the peak after heel strike for longer time when compared to the reference data. This might be because of the inaccuracy of motion from the robotic arm or from some other unknown source. The descent before toe-off is comparable to the human ankle's data.
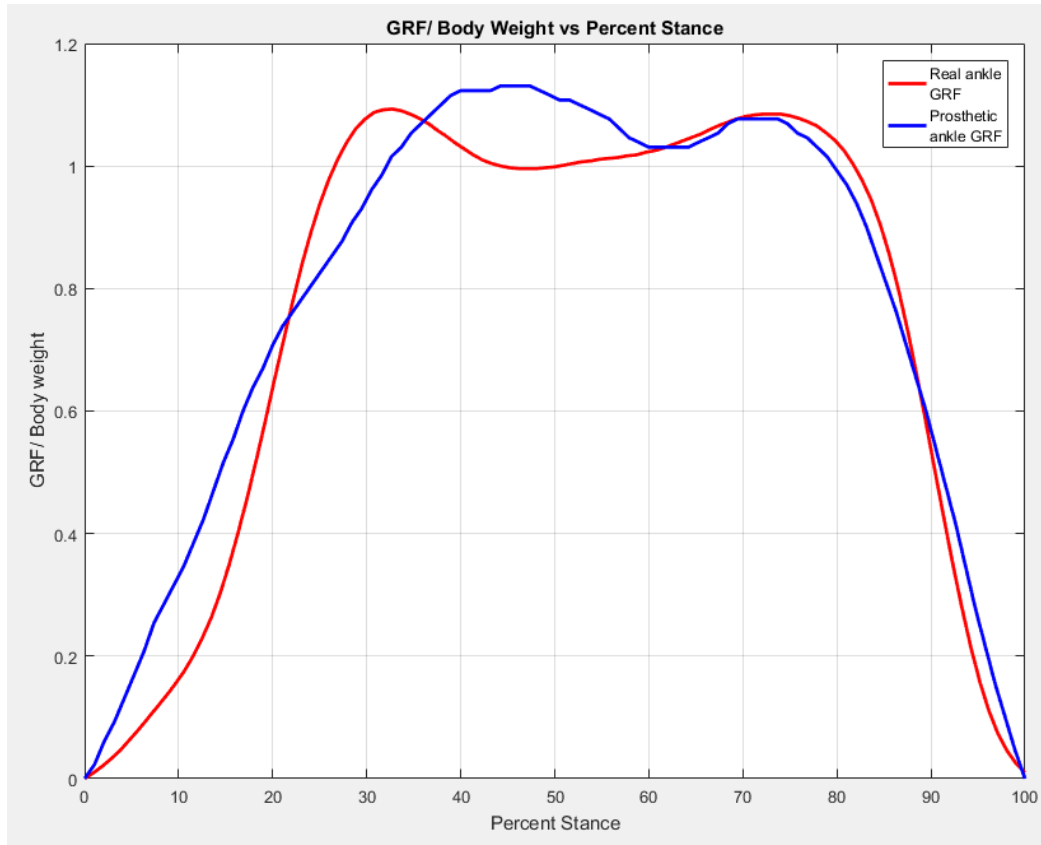
Figure 41. Comparison Between Ground Reaction Forces of The Human Ankle (Red) and The Prosthetic Ankle (Blue).

The data and the observations from the above experiment was used to decide the feasibility of the prosthetic ankle design. The results showed that the design supported the user while walking and could be used as a prosthetic ankle. The next section will discuss the setup and results of the second experiment.

3.2 Second Test

3.2.1. Aim

The aim of the experiment was to compare various aspects of the prosthetic ankle with a human ankle. In this experiment, the prosthetic ankle was tested and ankle angle and moment data were collected. The data was compared to the reference data from Figure 12.

3.2.2. Setup

A glass infused nylon 3D printed ankle was used for the experiment. The test was performed on an able-bodied human wearing a hands-free walking crutch. iWALK is a crutch used for leg injury rehabilitation. It used a stump for the ankle. This stump was replaced by the passive prosthetic ankle with an adapter attached to it instead of the mounting pyramid. The assembled ankle can be seen in Figure 42. This assembly was attached to the iWALK crutch as seen in Figure 43. This made the rig ready to be worn by the subject. The iWALK was fastened using bands on the crutch. The subject was wearing the crutch while collecting data for the experiment.

Figure 42. The Ankle with Custom Made Adapter For I-Walk
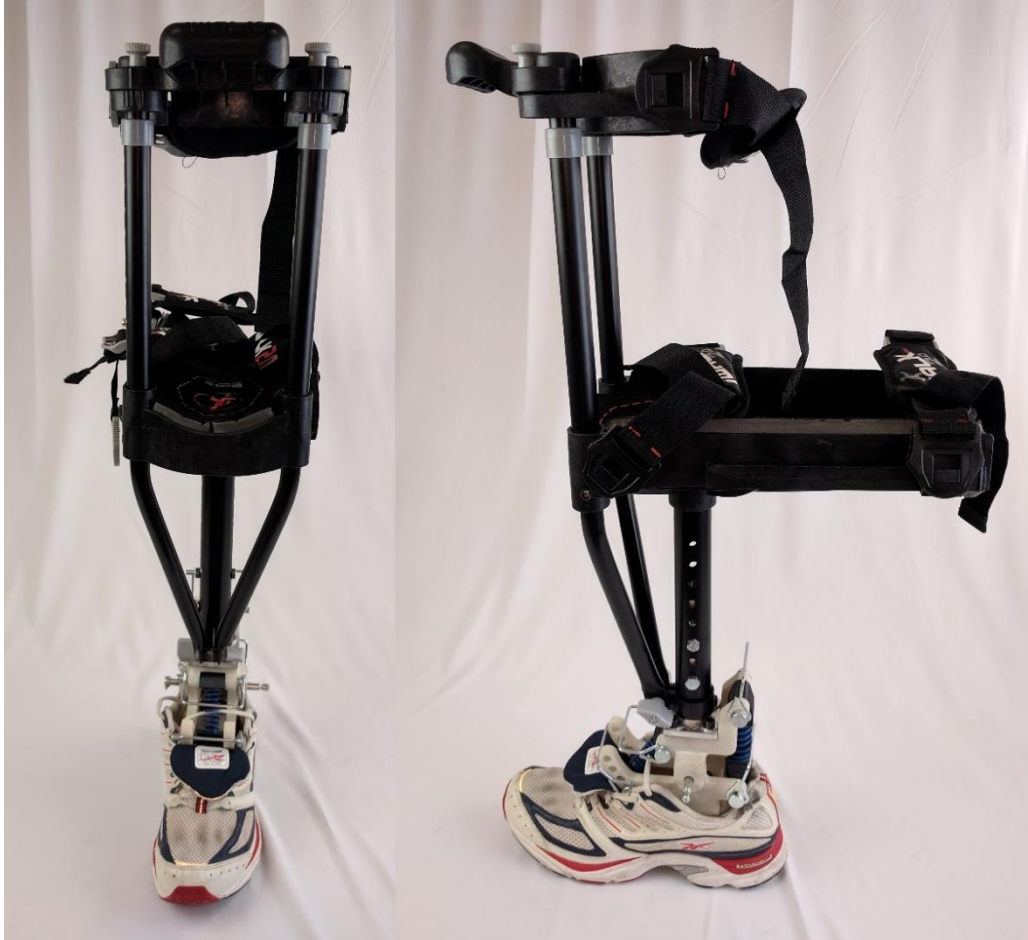
Figure 43. Assembled Testing Rig

The experiment was performed in a gait lab fully equipped for motion capture. A Vicon motion capture system was used to collect data. The system had eleven cameras pointed towards the treadmill. The treadmill is a Bertec Instrumented Treadmill. It has GRF sensors and velocity and acceleration control on either side. The motion capture system uses reflective markers to detect motion. The trajectory of each marker is captured. The markers were positioned at certain locations with the software pre-programmed to calculate data from the capture. Vicon Nexus 2 software was used to post-process data captured during the experiment. After post-processing, the angle and moment was calculated. The next section recounts the procedure of the experiment.

42

3.2.3. Experimentation

The subject wore the crutch with the passive ankle attached. The subject walked on the treadmill while also wearing a harness to prevent the subject from falling. The treadmill was set at 0.5 m/s walking speed which was lower than normal walking speed. The speed was lowered because the subject was not accustomed to walking with a crutch and higher speeds could cause the subject to topple. The subject walked on the treadmill two times for 30 seconds each. The subject's motion was captured and post-processed. The capture usually has many gaps in the data so post-processing was used with spline algorithm to fill the gaps. After post-processing the trajectories, angle and moment data were collected from the software and averaged. Data for a total of 16 steps were processed. These results and their significance will be discussed in the next section.

3.2.4. Results and Observations

Figure 44 shows the angle vs gait cycle data for the 16 steps, their average and the human ankle reference taken from Figure 12. It can be seen from the graph that at heel strike (H.S.) the prosthetic ankle does not dorsiflex as much as the human ankle leading to lower energy absorption. The peak of the averaged curve is higher than that of the reference data. This should lead to higher push-off energy during toe-off (T.O.) but due to the device's design and the stiffness of the springs used, it does not dorsiflex further than the equilibrium point. This decreases the push-off power delivered by the system. The higher ankle angle results in higher moment in the ankle.
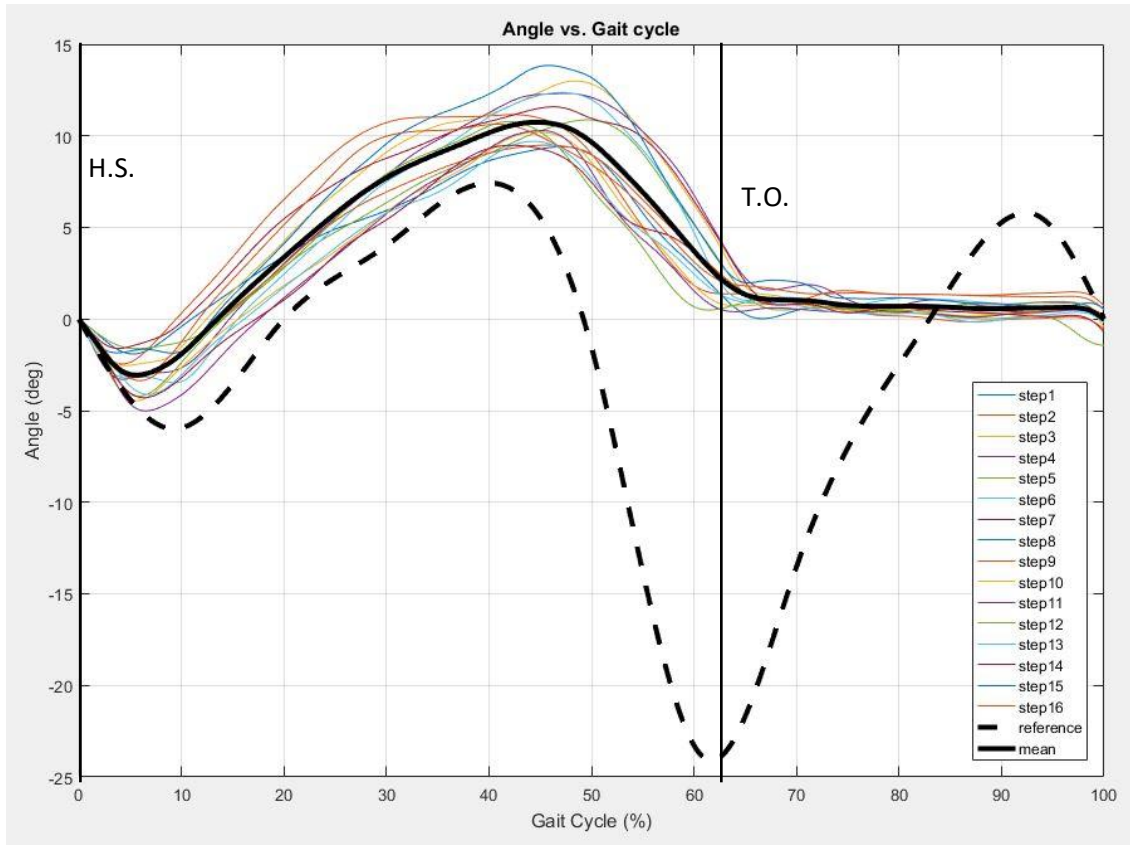
Figure 44. Angle Vs. Gait Cycle for The Prosthetic Ankle with The Reference Data

The moment of the prosthetic ankle depended on the ankle angle because of the springs delivering most of the moment. Figure 45 shows the moment vs gait cycle data for the ankle. The moment is averaged over 16 steps. There was noise in the moment data because of the irregular GRF data from the force plate. This noise in the moment data was smoothened using 9th order polynomial curve fit. The data was plotted as in Figure 45. As seen in the figure, due to the lower dip in ankle angle after H.S., the negative moment area is smaller than the reference data. The moment peaks right after that and plateaus for some time. At T.O., the moment dips to negative, unlike the reference data. The effectiveness of the design proposed can be seen in the phase diagram as discussed below.

44
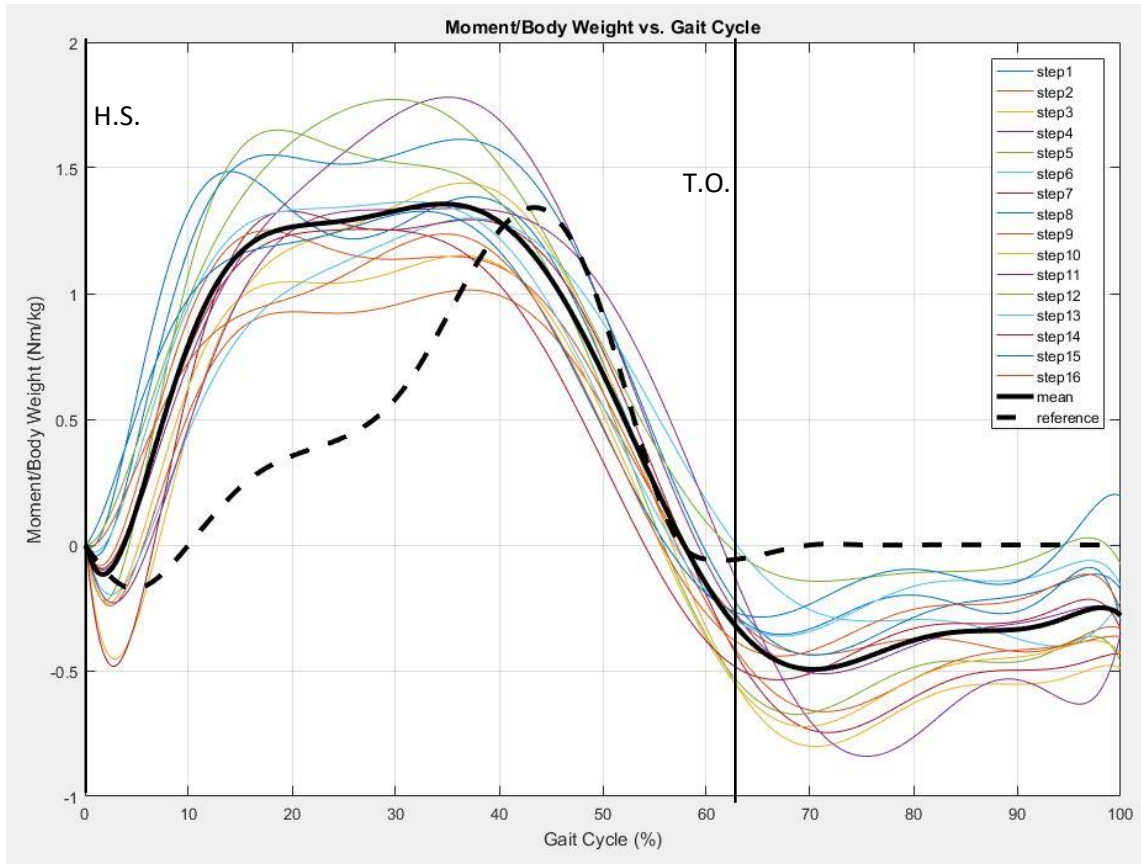
Figure 45. Moment Per Body Weight Vs. Gait Cycle for The Prosthetic Ankle with The Reference Data

The phase diagram shown in Figure 46 was plotted based on the average data from the angle and moment graphs. Here it can be seen that the ankle, in spite being passive, closely mimics the human ankle. With proper tuning, the gait with the proposed design would be able to imitate able bodied human gait.
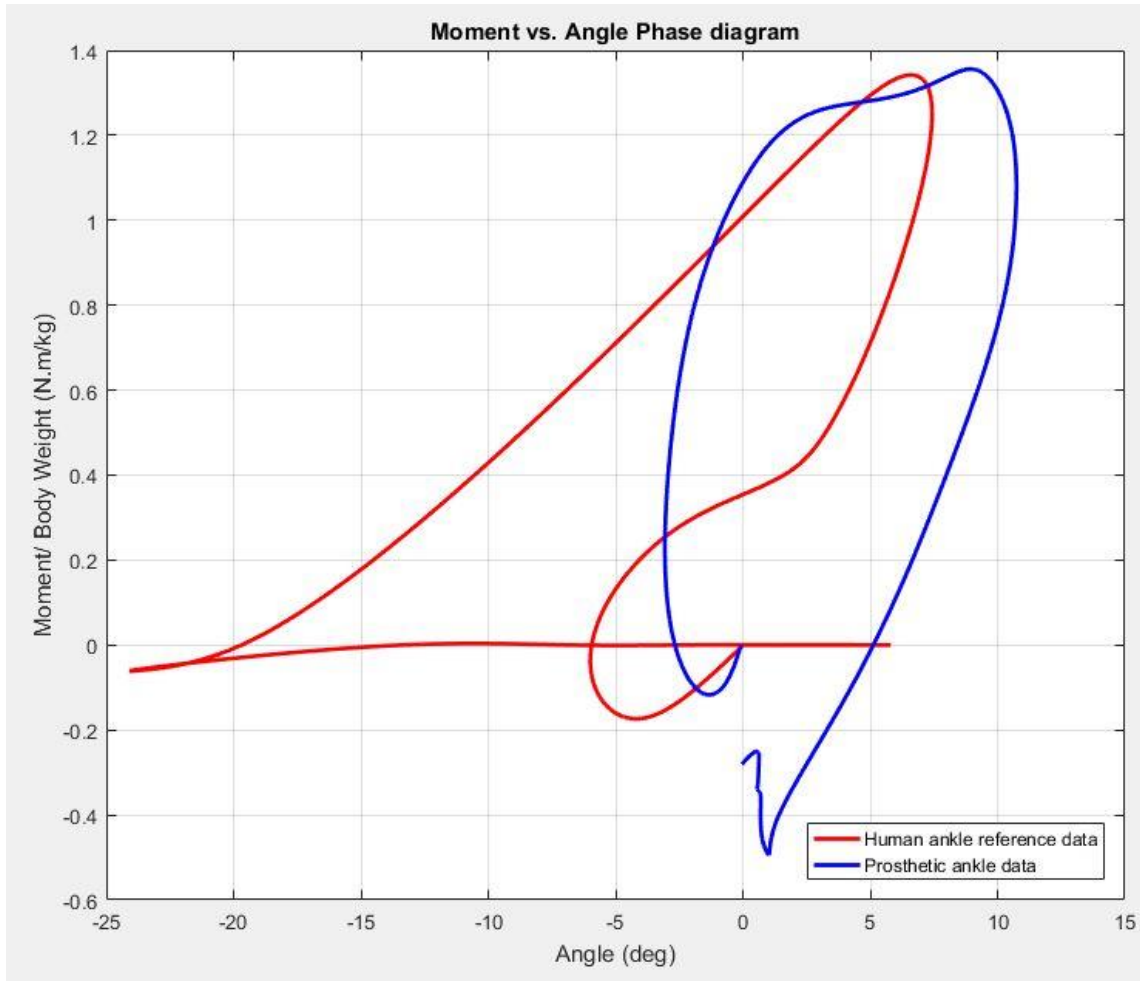
Figure 46. Phase Diagram Comparing Human Ankle Data and The Passive Prosthetic Ankle Data

The experiments discussed above point towards the fact that the design proposed in this thesis is closer to a human ankle than the SACH foot. The task now is to see the effect of the ankle on the healthy leg of an amputee. A biomechanics simulation software is used for this analysis. Its procedure, development, etc. are discussed in the next chapter.

CHAPTER 4

OPENSIM SIMULATION

OpenSim is a simulation platform used for biomechanical systems. It is used for modelling, simulation, and analysis of various biomechanical systems with support for optical tracking data. Being open source, its source code and files can be altered easily to fit the need of the project. OpenSim uses an '.xml' file type which is easy to program and use. It is a very effective tool to check the effects of a prosthetic ankle on the able leg. The method used to perform the analysis is described below.

4.1 Modelling of The Prosthetic Ankle

To model the analysis, '.stl' files of the prosthesis were included in an existing file. This existing file was a human body model available in the examples of the software. The right leg files were replaced with the STL files of the solid model for the prosthetic ankle. The muscles were replaced with springs and the parameters were set. The code was modified to perform the analysis. APPENDIX A consists the modifications made to the code used to simulate the ankle. Figure 47 shows a still of the model from the OpenSim simulation. A stump was attached to the amputated right leg which then attached to the part B of the ankle. The foot and the part A of the ankle formed a single piece in place of the human foot. Three contact geometry spheres were placed on the foot of the prosthetic along with the ground platform. These geometries provided contact forces when the model performed gait.
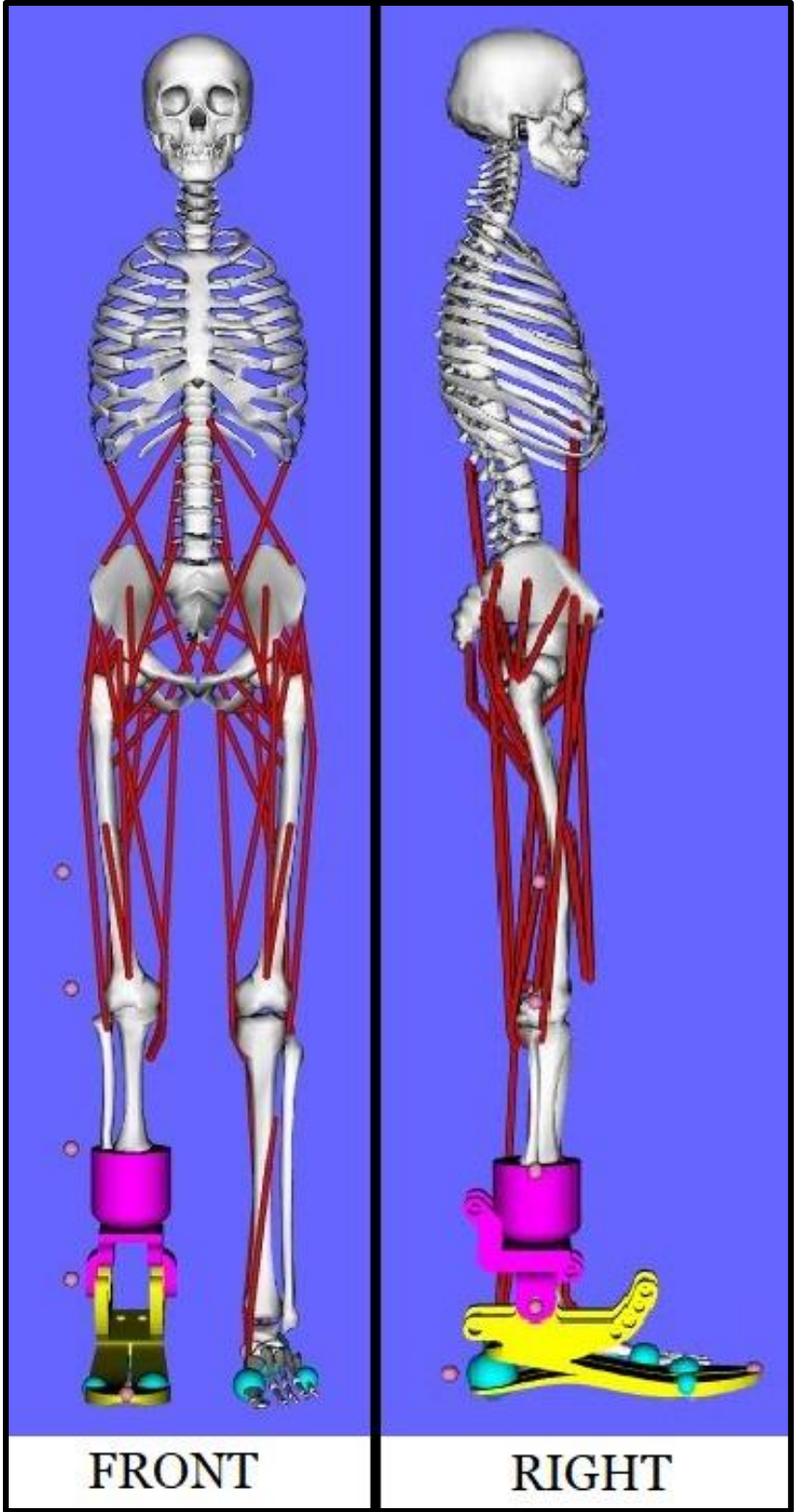
Figure 47. Opensim Model for A Human Amputee with The Prosthetic Ankle
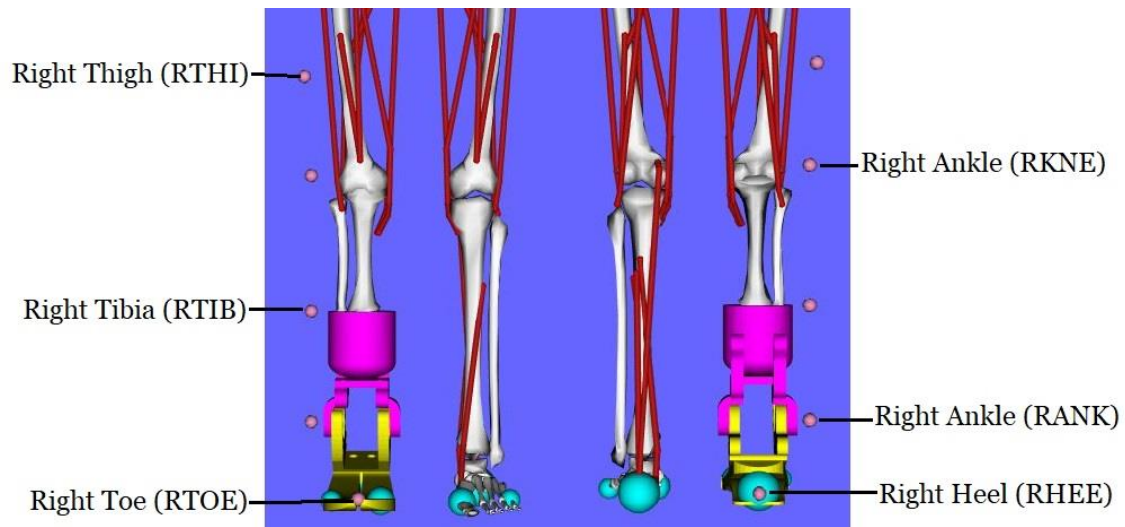
Figure 48. Optical Tracking Markers with Their Labels

Table 2. Marker name and placement list (Vicon Nexus 2.5 Documentation 2017)

Marker name	Location	Marker Placement
RTHI	Right thigh	Over the Upper lateral 1/3 surface of the right thigh
RKNE	Right knee	On the flexion-extension axis of the right knee
RTIB	Right tibia	Over the upper 1/3 surface of the right shank
RANK	Right ankle	On the lateral malleolus along an imaginary line that passes through the transmalleolar axis
RHEE	Right heel	On the calcaneus at the same height above the plantar surface of the foot as the toe marker
RTOE	Right toe	Over the second metatarsal head, on the mid-foot side of the equinus break between fore-foot and mid-foot

To emulate the motion of the subject's ankle from section 3.2.4 Second Test, markers were placed on the model. These markers were placed in relation to the motion capture markers. Figure 48 shows the location of the markers in OpenSim. Table 2 describes the exact location of the markers as taken from the Vicon Nexus motion capture system documentation (Vicon Nexus 2.5 Documentation 2017).

4.2 Simulation with Marker Data

After setting up the model, the simulation was run. Figure 49 shows the prosthetic's gait. The simulation consists of a single gait cycle for the prosthetic leg. The prosthetic leg in the simulation follows the motion of the test rig from the experiment due to the markers. It should be noted that the knee angles were exaggerated in the simulation as the knee did not bend as much during the experiment. This simulation was used to obtain the tendon actuation and force data for the subject. This data will be discussed in the next section.

4.3 Results

To analyze the actutaion of muscles in the amputated leg, data of the same muscles from right (amputated) and left (able) leg were plotted. One muscle was selected from the anterior and the posterior thigh for analysis. After refering some research articles (Q.Liu, et al. 2006), Biceps Femoris Long Head (BFLH) and Vastus Intermedius (VI) were selected. BFLH is responsible for the extension of the knee joint while the VI group is responsible for the flexion of the knee joint. Figure 50 shows the plotted data for these muscle and tendon groups. It was evident from the plot that the right and left leg actuation was different for the gait. The left BFLH can be observed to have higher range of forces/actuation than the right BFLH. While the right VI almost flat lined in comparison to the range of forces of the left VI. This might be because of the test rig and not the result of the prosthetic ankle.

50

It would be interesting to check the output of the analysis with an amputee wearing the ankle. This test would take a lot of resources and time. It will be something done in the future. All the data obtained by such an experiment will be better than the data discussed above in the thesis.
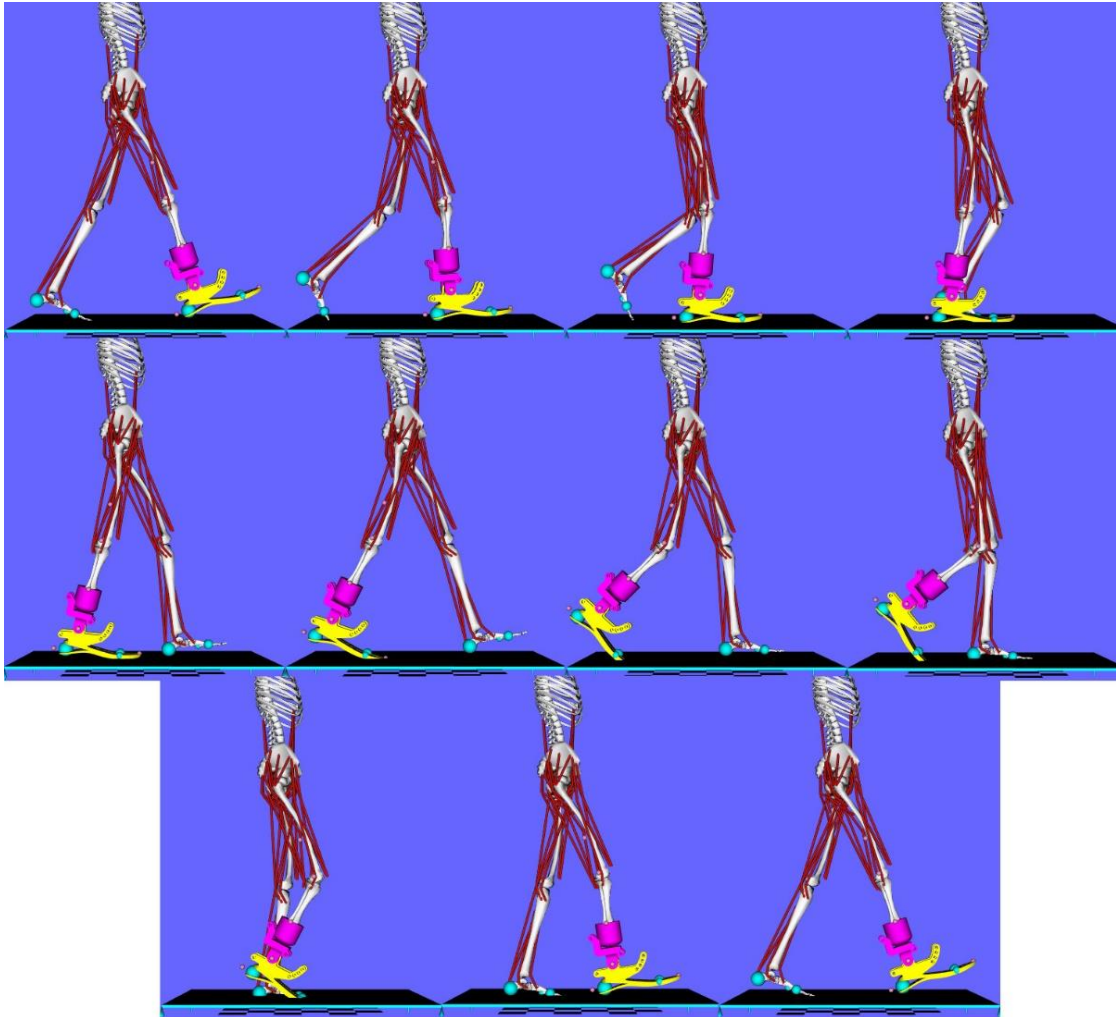
Figure 49. Simulation of Prosthetic Gait in Opensim
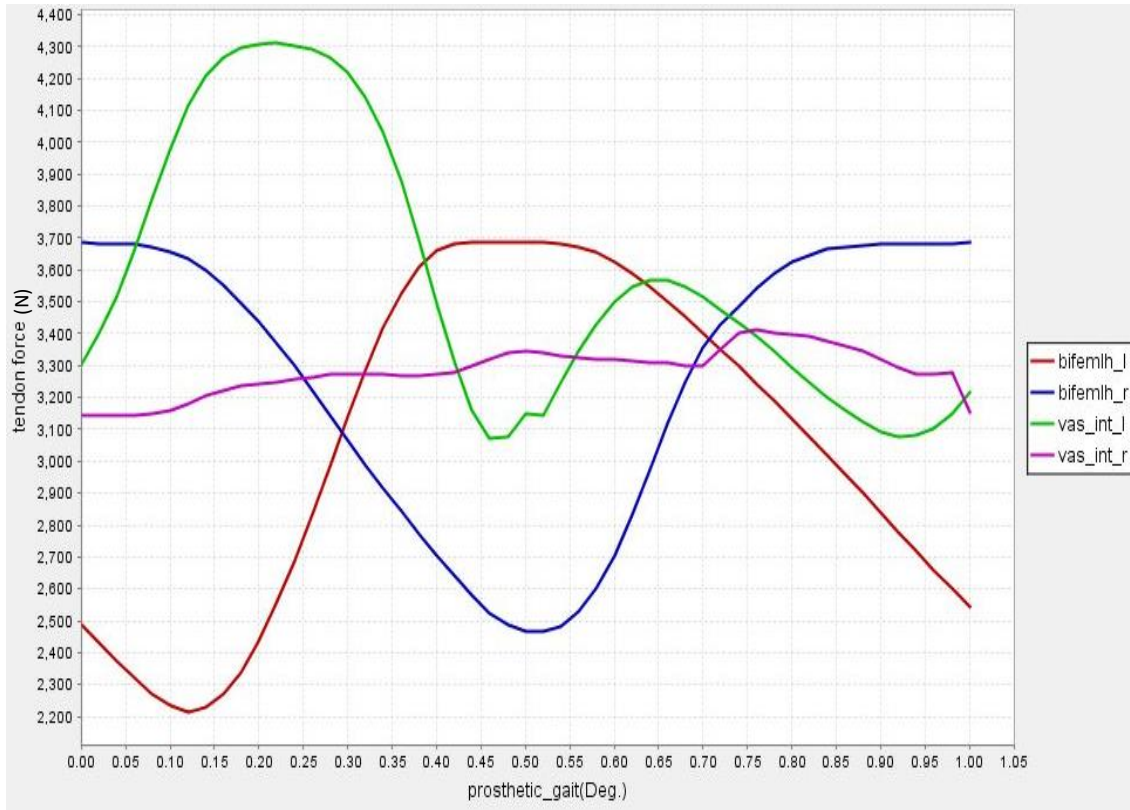
Figure 50. Comparison of Able Leg (Left) and Amputated Leg (Right) from The Simulation.

CHAPTER 5

CONCLUSION

In this work, a passive prosthetic ankle was designed and developed using simulations and analysis. The ankle was manufactured and tested on various. The results from these experiments were discussed. The ankle design was found to work well in the situations tested. A simulation was conducted to check the biomechanical effects of the prosthesis on the residual muscles of the amputee. It was observed that a prosthesis can affect the range of forces in the leg muscles and tendons. Below, some improvements to the existing design and the future experimentation plans are discussed.

5.1 Future Work

The design discussed in the thesis above is capable of walking on level ground. But it fails on slopes. The next step in improving the design is to modify the existing design to allow it to work on slopes. Figure 51 shows the rendered image of the improved design. The new design incorporates cam follower mechanism into the ankle's design. The Cam-follower are designed to be friction surfaces, with a small gap between the two. This gap allows the user to apply body weight onto the ankle and set the angle of the foot with respect to the walking surface. After the cam and follower come into contact, they roll over each other and perform the gait. When the swing phase starts, the ankle resets and goes back to its original position. The springs will be welded to the spring mount for rigid support during compression and extension of the spring. The slot on the upper part of the prosthetic ankle will have an oblong bearing to provide smooth motion. All the parts are held together using grooved shafts and retaining rings. Figure 52 shows the cross-sectional view of the ankle where the cam follower mechanism can be seen.
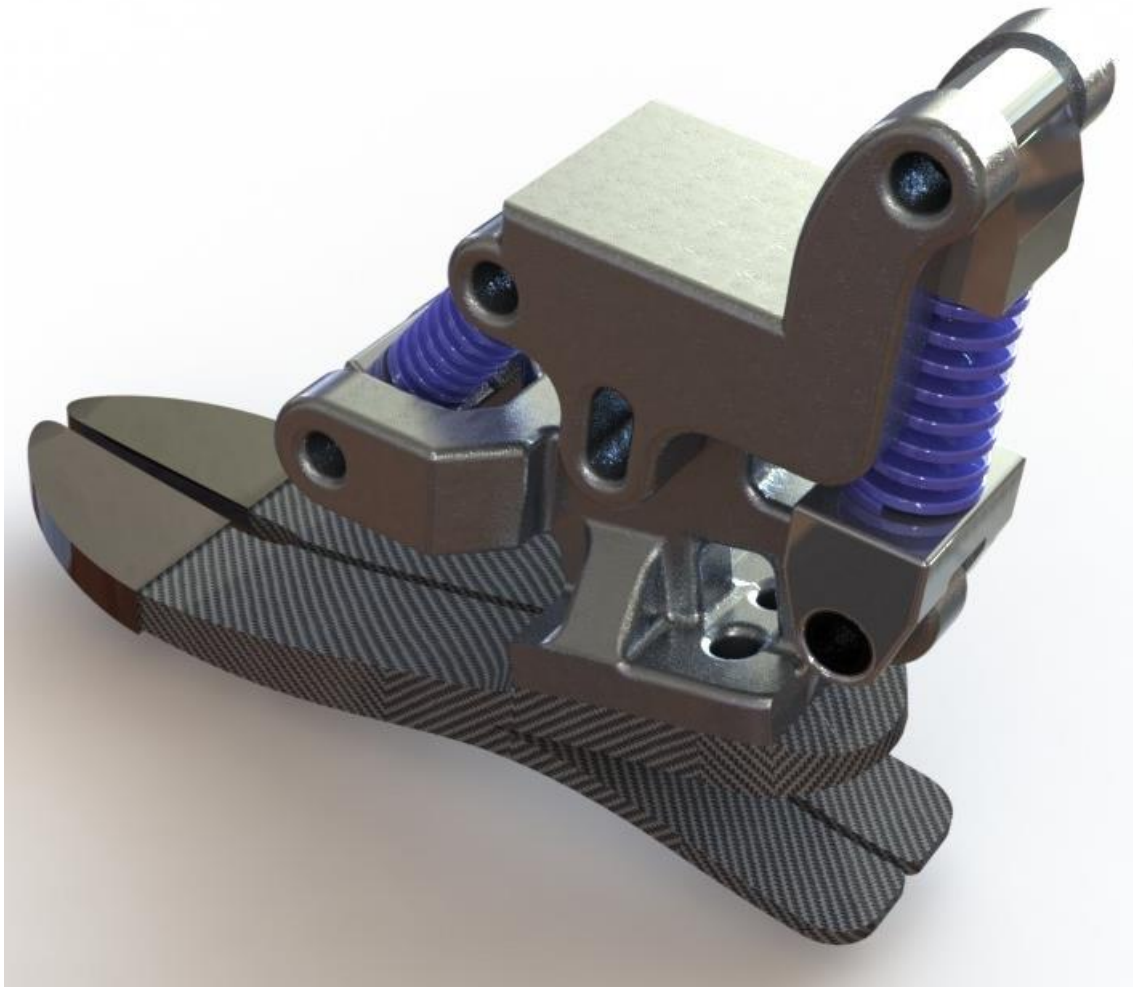
Figure 51. CAD for Slope Adaptable Ankle
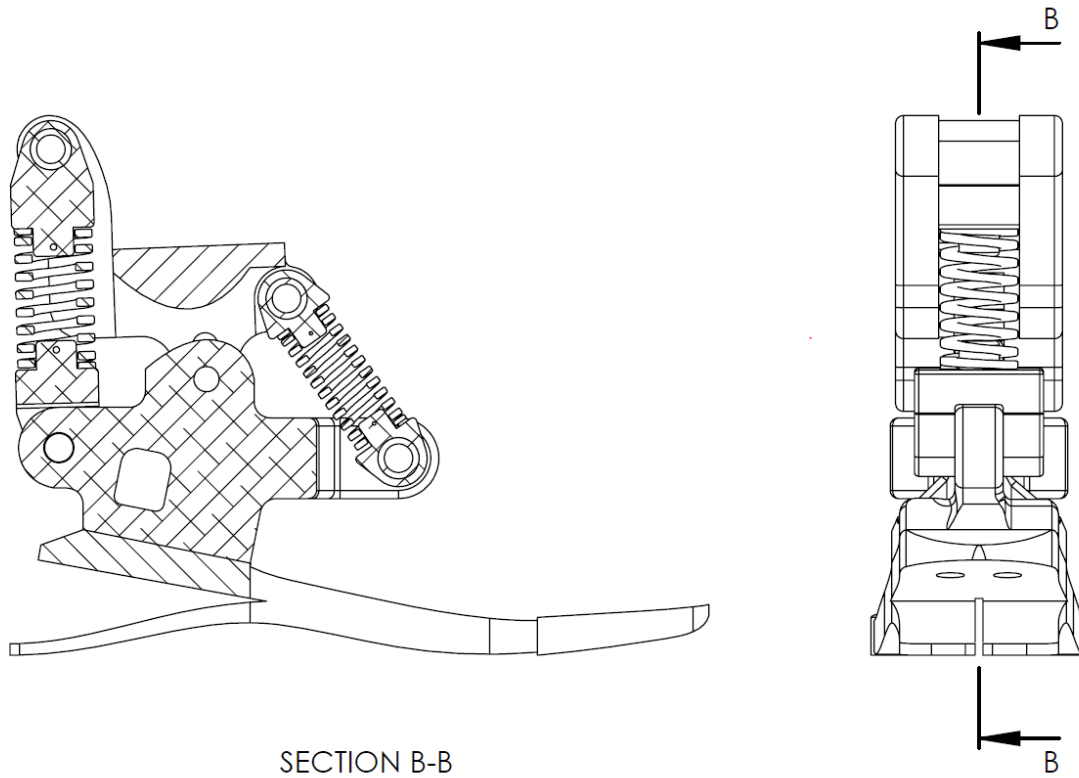
SECTION B-B

Figure 52. Cross Sectional View of The Cam Mechanism

All the above discussed details indicate that the design can be improved, more experiments would help validate the design. But, the simple design presented in this thesis has proven to be useful and a significant step forward in the direction of achieving a truly bionic prosthesis.

REFERENCES

Amiot, David E., et al. "Development of a passive and slope adaptable prosthetic foot." IDETC/CIE. Cleveland, Ohio, USA: ASME , 2017. 1-9.

Arms. 2015. http://sdk.rethinkrobotics.com/wiki/Arms.

Baxter. 2008. http://www.rethinkrobotics.com/baxter/.

Brackx, Branko, Michaël Van Damme, Arnout Matthys, Bram Vanderborght, and Dirk Lefeber. "Passive Ankle-Foot Prosthesis Prototype with Extended Push-Off ." International Journal of Advanced Robotic Systems, 2012: 1-9.

Chowdhury, Subhra, and Neelesh Kumar. "Estimation of Forces and Moments of Lower Limb Joints from." Journal of Rehabilitation Robotics, 2013: 93-98.

Garber, Megan. The Atlantic. November 21, 2013. https://www.theatlantic.com/technology/archive/2013/11/the-perfect-3-000-year-old-toe-a-brief-history-of-prosthetic-limbs/281653/.

Go, Shane. Time Toast. 2015. https://www.timetoast.com/timelines/prosthetics-04797506-d5e3-477d-bb68-812435358ec2.

Hansen, Andrew H., Dudley S. Childress, and Steve C. Miff. "Roll-over characteristics of human walking on inclined surfaces." Human Movement Science, 2004: 807-821.

Hitt, Joseph Karl. A ROBOTIC TRANSTIBIAL PROSTHESIS WITH REGENERATIVE KINETICS. Phoenix: Arizona State University, 2008.

Jaipur Leg. July 1, 2017. https://en.wikipedia.org/wiki/Jaipur_leg.

Jaipurfoot.org. 2016. http://www.jaipurfoot.org/03_Technology_history.asp.

KathrynZiegler-Graham, Ellen J.MacKenzie, Patti L.Ephraim, Thomas G.Travison, and RonBrookmeyer. "Estimating the Prevalence of Limb Loss in the United States: 2005 to 2050." Archives of Physical Medicine and Rehabilitation, 2008: 422-428.

Koelewijn, Anne, and Antonie J. van den Bogert. INFLUENCE OF STIFFNESS OF AN ANKLE-FOOT ORTHOSIS ON GAIT. Cleveland, OH: The American Society of Biomechanincs, n.d.

Leclair, Justin. DEVELOPMENT AND TESTING OF AN UNPOWERED ANKLE EXOSKELETON FOR WALKING ASSIST. Masters Thesis, Ottawa, Canada: University of Ottawa, 2016.

MF, Owings, and Kozak LJ. "Ambulatory and inpatient procedures in the United States, 1996." Vitaland Health Statistics, 1998: 1-119.

Mooney, Luke M., Cara H. Lai, and Elliott J. Rouse. "Design and Characterization of a Biologically Inspired QuasiPassive." Engineering in Medicine and Biology Society . Chicago, IL, USA: IEEE, 2014. 1611-1617.

Nguyen, Tan Thang, Thanh-Phong Dao, and Shyh-Chour Huang. "BIOMECHANICAL DESIGN OF A NOVEL SIX DOF COMPLIANT PROSTHETIC ANKLE-FOOT 2.0 FOR REHABILITATION OF AMPUTEE." International Design Engineering Technical Conferences and Computers and Information in Engineering Conference. Cleveland, Ohio, USA: ASME, 2017. 1-7.

Nickel, Eric, Jonathon Sensinger, and Andrew Hansen. "Passive prosthetic ankle-foot mechanism for automatic adaptation to." Journal of Rehabilitation Research & Development, 2014: 803-814.

Ossur Americas. Pro-Flex Product Page. 2017. https://www.ossur.com/prosthetic-solutions/products/dynamic-solutions/pro-flex (accessed October 10, 2017).

P.Procter, and J.P.Paul. "Ankle joint biomechanics." Journal of Biomechanics 15, no. 9 (1982): 627-634.

PITKIN, M. "What can normal gait biomechanics teach a designer of lower." Acta Bioeng Biomech., 2013.

Q.Liu, May, Frank C.Anderson, Marcus G.Pandy, and Scott L.Delp. "Muscles that support the body also modulate forward progression during walking." Journal of Biomechanics, 2006: 2623-2630.

Rihs, Daniel, and Ivan Polizzi. Prosthetic Foot Design. Final year Project Report, Melbourne, Victoria, Australia: Monash University, 2001.

Varela, Maria João, Marco Ceccarelli, and Paulo Flores. "A kinematic characterization of human walking by." Mechanism and Machine Theory, 2015: 125-139.

Vicon Nexus 2.5 Documentation. "Lower body modelling with Plug in Gait." Vicon. 2017. https://docs.vicon.com/display/Nexus25/Lower+body+modeling+with+Plug-in+Gait.

Vrieling, A.H., H.G. van Keeken, T. Schoppen, and E. Otten. "Uphill and downhill walking in unilateral lower limb amputees." Gait Posture, 2008: 235-242.

Whittle, Michael W. Gait Analysis An Introduction. Elsevier Ltd., 2007.

Williams, Ryan J., Andrew H. Hansen, and Steven A. Gard. "Prosthetic Ankle-Foot Mechanism Capable of Automatic Adaptation to the Walking Surface." Journal of Biomechanical Engineering, 2009: 035002.

Zeng, Yadan. "Design And Testing Of A Passive Prosthetic Ankle With Mechanical Performance Similar To That Of A Natural Ankle." epublications.marquette, January 1, 2013.

APPENDIX A

OPENSIM MODEL GENERATION CODE

The code snippet below is the modification/addition to the code of "gait2354_simbody.osim" which is included in the software example files. The code below is useless without the parent code. All rights to the original code reserved to the original authors credited at the bottom of the code snippet.

```
<Body name="tibia_r">

<mass>3.7075</mass>

<mass_center> 0 -0.1867 0</mass_center>

 <inertia_xx>0.0504</inertia_xx>

 <inertia_yy>0.0051</inertia_yy>

 <inertia_zz>0.0511</inertia_zz>

 <inertia_xy>0</inertia_xy>

 <inertia_xz>0</inertia_xz>

 <inertia_yz>0</inertia_yz>

<!--Joint that connects this body with the parent body.-->

<Joint>

<CustomJoint name="knee_r">

 <!--Name of the parent body to which this joint connects its owner body.-->

 <parent_body>femur_r</parent_body>

 <!--Location of the joint in the parent body specified in the parent reference frame.
Default is (0,0,0).-->
```

```xml
<location_in_parent>0 0 0</location_in_parent>
```

<!--Orientation of the joint in the parent body specified in the parent reference frame. Euler XYZ body-fixed rotation angles are used to express the orientation. Default is (0,0,0).-->

```xml
<orientation_in_parent>0 0 0</orientation_in_parent>
```

<!--Location of the joint in the child body specified in the child reference frame. For SIMM models, this vector is always the zero vector (i.e., the body reference frame coincides with the joint). -->

```xml
<location>0 0 0</location>
```

<!--Orientation of the joint in the owing body specified in the owning body reference frame. Euler XYZ body-fixed rotation angles are used to express the orientation. -->

```xml
<orientation>0 0 0</orientation>
```

<!--Set holding the generalized coordinates (q's) that parmeterize this joint.-->

```xml
<CoordinateSet>
```

```xml
<objects>
```

```xml
<Coordinate name="knee_angle_r">
```

<!--Coordinate can describe rotational, translational, or coupled motion. Defaults to rotational.-->

```xml
<motion_type>rotational</motion_type>
```

<!--The value of this coordinate before any value has been set. Rotational coordinate value is in radians and Translational in meters.-->

```xml
<default_value>0</default_value>
<!--The speed value of this coordinate before any value has been set. Rotational
coordinate value is in rad/s and Translational in m/s.-->
<default_speed_value>0</default_speed_value>
<!--The minimum and maximum values that the coordinate can range between.
Rotational coordinate range in radians and Translational in meters.-->
<range>-2.0943951 0.17453293</range>
<!--Flag indicating whether or not the values of the coordinates should be limited to the
range, above.-->
<clamped>false</clamped>
<!--Flag indicating whether or not the values of the coordinates should be constrained
to the current (e.g. default) value, above.-->
<locked>false</locked>
<!--If specified, the coordinate can be prescribed by a function of time. It can be any
OpenSim Function with valid second order derivatives.-->
<prescribed_function />
<!--Flag indicating whether or not the values of the coordinates should be prescribed
according to the function above. It is ignored if the no prescribed function is specified.-->
<prescribed>false</prescribed>
</Coordinate>
</objects>
```

```xml
<groups />

</CoordinateSet>

<!--Whether the joint transform defines parent->child or child->parent.-->

<reverse>false</reverse>

<!--Defines how the child body moves with respect to the parent as a function of the generalized coordinates.-->

<SpatialTransform>

<!--3 Axes for rotations are listed first.-->

<TransformAxis name="rotation1">

<!--Names of the coordinates that serve as the independent variables     of the transform function.-->

<coordinates>knee_angle_r</coordinates>

<!--Rotation or translation axis for the transform.-->

<axis>0 0 1</axis>

<!--Transform function of the generalized coordinates used to     represent the amount of transformation along a specified axis.-->

<function>

<LinearFunction>

<coefficients> 1 0</coefficients>

</LinearFunction>
```

```xml
    </function>

  </TransformAxis>

  <TransformAxis name="rotation2">

  <!--Names of the coordinates that serve as the independent variables      of the
transform function.-->

  <coordinates></coordinates>

  <!--Rotation or translation axis for the transform.-->

  <axis>0 1 0</axis>

  <!--Transform function of the generalized coordinates used to      represent the
amount of transformation along a specified axis.-->

  <function>

  <Constant>

  <value>0</value>

  </Constant>

  </function>

  </TransformAxis>

  <TransformAxis name="rotation3">

  <!--Names of the coordinates that serve as the independent variables      of the
transform function.-->

  <coordinates></coordinates>
```

```xml
<!--Rotation or translation axis for the transform.-->

<axis>1 0 0</axis>

<!--Transform function of the generalized coordinates used to      represent the
amount of transformation along a specified axis.-->

<function>

<Constant>

<value>0</value>

</Constant>

</function>

</TransformAxis>

<!--3 Axes for translations are listed next.-->

<TransformAxis name="translation1">

<!--Names of the coordinates that serve as the independent variables      of the
transform function.-->

<coordinates>knee_angle_r</coordinates>

<!--Rotation or translation axis for the transform.-->

<axis>1 0 0</axis>

<!--Transform function of the generalized coordinates used to      represent the
amount of transformation along a specified axis.-->

<function>
```

```xml
<SimmSpline>

<x> -2.0944 -1.74533 -1.39626 -1.0472 -0.698132 -0.349066 -0.174533 0.197344 0.337395 0.490178 1.52146 2.0944</x>

<y> -0.0032 0.00179 0.00411 0.0041 0.00212 -0.001 -0.0031 -0.005227 -0.005435 -0.005574 -0.005435 -0.00525</y>

</SimmSpline>

</function>

</TransformAxis>

<TransformAxis name="translation2">

<!--Names of the coordinates that serve as the independent variables      of the transform function.-->

<coordinates>knee_angle_r</coordinates>

<!--Rotation or translation axis for the transform.-->

<axis>0 1 0</axis>

<!--Transform function of the generalized coordinates used to      represent the amount of transformation along a specified axis.-->

<function>

<SimmSpline>

<x> -2.0944 -1.22173 -0.523599 -0.349066 -0.174533 0.159149 2.0944</x>

<y> -0.4226 -0.4082 -0.399 -0.3976 -0.3966 -0.395264 -0.396</y>
```

```xml
        </SimmSpline>

      </function>

    </TransformAxis>

    <TransformAxis name="translation3">

      <!--Names of the coordinates that serve as the independent variables      of the
transform function.-->

      <coordinates></coordinates>

      <!--Rotation or translation axis for the transform.-->

      <axis>0 0 1</axis>

      <!--Transform function of the generalized coordinates used to      represent the
amount of transformation along a specified axis.-->

      <function>

      <Constant>

      <value>0</value>

      </Constant>

      </function>

    </TransformAxis>

    </SpatialTransform>

    </CustomJoint>

    </Joint>
```

<VisibleObject>

<!--Set of geometry files and associated attributes, allow .vtp, .stl, .obj-->

<GeometrySet>

<objects>

<DisplayGeometry>

<!--Name of geometry file .vtp, .stl, .obj-->

<geometry_file>tibia.vtp</geometry_file>

<!--Color used to display the geometry when visible-->

<color> 1 1 1</color>

<!--Name of texture file .jpg, .bmp-->

<texture_file />

<!--in body transform specified as 3 rotations (rad) followed by 3 translations rX rY rZ tx ty tz-->

<transform> -0 0 -0 0 0 0</transform>

<!--Three scale factors for display purposes: scaleX scaleY scaleZ-->

<scale_factors> 1 0.5 1</scale_factors>

<!--Display Pref. 0:Hide 1:Wire 3:Flat 4:Shaded-->

<display_preference>4</display_preference>

<!--Display opacity between 0.0 and 1.0-->

```
</DisplayGeometry>

<DisplayGeometry>

<!--Name of geometry file .vtp, .stl, .obj-->

<geometry_file>fibula.vtp</geometry_file>

<!--Color used to display the geometry when visible-->

<color> 1 1 1</color>

<!--Name of texture file .jpg, .bmp-->

<texture_file />

<!--in body transform specified as 3 rotations (rad) followed by 3 translations rX rY rZ
tx ty tz-->

 <transform> -0 0 -0 0 0 0</transform>

<!--Three scale factors for display purposes: scaleX scaleY scaleZ-->

<scale_factors> 1 0.5 1</scale_factors>

<!--Display Pref. 0:Hide 1:Wire 3:Flat 4:Shaded-->

<display_preference>4</display_preference>

<!--Display opacity between 0.0 and 1.0-->

<opacity>1</opacity>

</DisplayGeometry>

<DisplayGeometry>

<!--Name of geometry file .vtp, .stl, .obj-->
```

```xml
<geometry_file>mm2.stl</geometry_file>

<!--Color used to display the geometry when visible-->

<color> 1 0 1</color>

<!--Name of texture file .jpg, .bmp-->

<texture_file />

<!--in body transform specified as 3 rotations (rad) followed by 3 translations rX rY rZ
tx ty tz-->

<transform> -0 0 -0 -0.05 -0.3 -0.05</transform>

<!--Three scale factors for display purposes: scaleX scaleY scaleZ-->

<scale_factors> 0.1 0.05 0.1</scale_factors>

<!--Display Pref. 0:Hide 1:Wire 3:Flat 4:Shaded-->

<display_preference>4</display_preference>

<!--Display opacity between 0.0 and 1.0-->

<opacity>1</opacity>

</DisplayGeometry>

<DisplayGeometry>

<!--Name of geometry file .vtp, .stl, .obj-->

<geometry_file>ankle_2.stl</geometry_file>

<!--Color used to display the geometry when visible-->

<color> 1 0 1</color>
```

```xml
<!--Name of texture file .jpg, .bmp-->

<texture_file />

<!--in body transform specified as 3 rotations (rad) followed by 3 translations rX rY rZ
tx ty tz-->

<transform> -0 3.14 -0 0.0525 -0.4335 0.05625</transform>

<!--Three scale factors for display purposes: scaleX scaleY scaleZ-->

<scale_factors> 0.0015 0.0015 0.0015</scale_factors>

<!--Display Pref. 0:Hide 1:Wire 3:Flat 4:Shaded-->

<display_preference>4</display_preference>

<!--Display opacity between 0.0 and 1.0-->

<opacity>1</opacity>

</DisplayGeometry>

</objects>

<groups />

</GeometrySet>

<!--Three scale factors for display purposes: scaleX scaleY scaleZ-->

<scale_factors> 1 1 1</scale_factors>

<!--transform relative to owner specified as 3 rotations (rad) followed by 3 translations
rX rY rZ tx ty tz-->

<transform> -0 0 -0 0 0 0</transform>
```

```xml
<!--Whether to show a coordinate frame-->

<show_axes>false</show_axes>

<!--Display Pref. 0:Hide 1:Wire 3:Flat 4:Shaded Can be overriden for individual
geometries-->

<display_preference>4</display_preference>

</VisibleObject>

<WrapObjectSet>

<objects />

<groups />

</WrapObjectSet>

</Body>

        <Body name="bottom">

<mass>0.69</mass>

<mass_center> 0.046395 -0.063705 0</mass_center>

<inertia_xx>0.0014</inertia_xx>

<inertia_yy>0.0039</inertia_yy>

<inertia_zz>0.0041</inertia_zz>

<inertia_xy>0</inertia_xy>

<inertia_xz>0</inertia_xz>

<inertia_yz>0</inertia_yz>
```

```xml
<!--Joint that connects this body with the parent body.-->

<Joint>

<CustomJoint name="Pros_ankle_joint">

<!--Name of the parent body to which this joint connects its owner body.-->

<parent_body>tibia_r</parent_body>

<!--Location of the joint in the parent body specified in the parent reference frame.
Default is (0,0,0).-->

<location_in_parent>0 -0.363 0</location_in_parent>

<!--Orientation of the joint in the parent body specified in the parent reference frame.
Euler XYZ body-fixed rotation angles are used to express the orientation. Default is
(0,0,0).-->

<orientation_in_parent>0 0 0</orientation_in_parent>

<!--Location of the joint in the child body specified in the child reference frame. For
SIMM models, this vector is always the zero vector (i.e., the body reference frame
coincides with the joint). -->

<location>0 0 0</location>

<!--Orientation of the joint in the owing body specified in the owning body reference
frame.  Euler XYZ body-fixed rotation angles are used to express the orientation. -->

<orientation>0 0 0</orientation>

<!--Set holding the generalized coordinates (q's) that parmeterize this joint.-->

<CoordinateSet>
```

```xml
<objects>

<Coordinate name="hinge_angle">

<!--Coordinate can describe rotational, translational, or coupled motion. Defaults to
rotational.-->

<motion_type>rotational</motion_type>

<!--The value of this coordinate before any value has been set. Rotational coordinate
value is in radians and Translational in meters.-->

<default_value>0</default_value>

<!--The speed value of this coordinate before any value has been set. Rotational
coordinate value is in rad/s and Translational in m/s.-->

<default_speed_value>0</default_speed_value>

<!--The minimum and maximum values that the coordinate can range between.
Rotational coordinate range in radians and Translational in meters.-->

<range> -0.7854 0.7854</range>

<!--Flag indicating whether or not the values of the coordinates should be limited to the
range, above.-->

<clamped>false</clamped>

<!--Flag indicating whether or not the values of the coordinates should be constrained
to the current (e.g. default) value, above.-->

<locked>false</locked>
```

```xml
<!--If specified, the coordinate can be prescribed by a function of time. It can be any OpenSim Function with valid second order derivatives.-->
<prescribed_function />
<!--Flag indicating whether or not the values of the coordinates should be prescribed according to the function above. It is ignored if the no prescribed function is specified.-->
<prescribed>false</prescribed>
</Coordinate>
</objects>
<groups />
</CoordinateSet>
<!--Whether the joint transform defines parent->child or child->parent.-->
<reverse>false</reverse>
<!--Defines how the child body moves with respect to the parent as a function of the generalized coordinates.-->
<SpatialTransform>
<!--3 Axes for rotations are listed first.-->
<TransformAxis name="rotation1">
<!--Names of the coordinates that serve as the independent variables       of the transform function.-->
<coordinates>hinge_angle</coordinates>
```

<!--Rotation or translation axis for the transform.-->

<axis>0 0 0.1</axis>

<!--Transform function of the generalized coordinates used to   represent the amount of transformation along a specified axis.-->

<function>

<LinearFunction>

<coefficients> 1 0</coefficients>

</LinearFunction>

</function>

</TransformAxis>

<TransformAxis name="rotation2">

<!--Names of the coordinates that serve as the independent variables   of the transform function.-->

<coordinates></coordinates>

<!--Rotation or translation axis for the transform.-->

<axis>0 1 0</axis>

<!--Transform function of the generalized coordinates used to   represent the amount of transformation along a specified axis.-->

<function>

<Constant>

```xml
<value>0</value>

</Constant>

</function>

</TransformAxis>

<TransformAxis name="rotation3">

<!--Names of the coordinates that serve as the independent variables      of the
transform function.-->

<coordinates></coordinates>

<!--Rotation or translation axis for the transform.-->

<axis>1 0 0</axis>

<!--Transform function of the generalized coordinates used to      represent the
amount of transformation along a specified axis.-->

<function>

<Constant>

<value>0</value>

</Constant>

</function>

</TransformAxis>

<!--3 Axes for translations are listed next.-->

<TransformAxis name="translation1">
```

```xml
<!--Names of the coordinates that serve as the independent variables       of the
transform function.-->

<coordinates></coordinates>

<!--Rotation or translation axis for the transform.-->

<axis>1 0 0</axis>

<!--Transform function of the generalized coordinates used to       represent the
amount of transformation along a specified axis.-->

<function>

<Constant>

<value>0</value>

</Constant>

</function>

</TransformAxis>

<TransformAxis name="translation2">

<!--Names of the coordinates that serve as the independent variables       of the
transform function.-->

<coordinates></coordinates>

<!--Rotation or translation axis for the transform.-->

<axis>0 1 0</axis>
```

```xml
<!--Transform function of the generalized coordinates used to    represent the
amount of transformation along a specified axis.-->

<function>

<Constant>

<value>0</value>

</Constant>

</function>

</TransformAxis>

<TransformAxis name="translation3">

<!--Names of the coordinates that serve as the independent variables      of the
transform function.-->

<coordinates></coordinates>

<!--Rotation or translation axis for the transform.-->

<axis>0 0 1</axis>

<!--Transform function of the generalized coordinates used to    represent the
amount of transformation along a specified axis.-->

<function>

<Constant>

<value>0</value>

</Constant>
```

</function>

</TransformAxis>

</SpatialTransform>

</CustomJoint>

</Joint>

<VisibleObject>

<!--Set of geometry files and associated attributes, allow .vtp, .stl, .obj-->

<GeometrySet>

<objects>

<DisplayGeometry>

<!--Name of geometry file .vtp, .stl, .obj-->

<geometry_file>ankle_1.stl</geometry_file>

<!--Color used to display the geometry when visible-->

<color> 1 1 0</color>

<!--Name of texture file .jpg, .bmp-->

<texture_file />

<!--in body transform specified as 3 rotations (rad) followed by 3 translations rX rY rZ tx ty tz-->

<transform> -0 3.14 -0 0.13785 -0.0705 0.04125</transform>

<!--Three scale factors for display purposes: scaleX scaleY scaleZ-->

```xml
<scale_factors> 0.0015 0.0015 0.0015</scale_factors>

<!--Display Pref. 0:Hide 1:Wire 3:Flat 4:Shaded-->

<display_preference>4</display_preference>

<!--Display opacity between 0.0 and 1.0-->

<opacity>1</opacity>

</DisplayGeometry>

<DisplayGeometry>

<!--Name of geometry file .vtp, .stl, .obj-->

<geometry_file>Carbon_foot.stl</geometry_file>

<!--Color used to display the geometry when visible-->

<color> 1 1 0</color>

<!--Name of texture file .jpg, .bmp-->

<texture_file />

<!--in body transform specified as 3 rotations (rad) followed by 3 translations rX rY rZ
tx ty tz-->

<transform> -0 1.57 -0 -0.07415 -0.12645 0.0582</transform>

<!--Three scale factors for display purposes: scaleX scaleY scaleZ-->

<scale_factors> 0.0015 0.0015 0.0015</scale_factors>

<!--Display Pref. 0:Hide 1:Wire 3:Flat 4:Shaded-->

<display_preference>4</display_preference>
```

```xml
<!--Display opacity between 0.0 and 1.0-->

<opacity>1</opacity>

</DisplayGeometry>

</objects>

<groups />

</GeometrySet>

<!--Three scale factors for display purposes: scaleX scaleY scaleZ-->

<scale_factors> 1 1 1</scale_factors>

<!--transform relative to owner specified as 3 rotations (rad) followed by 3 translations
rX rY rZ tx ty tz-->

<transform> -0 0 -0 0 0 0</transform>

<!--Whether to show a coordinate frame-->

<show_axes>false</show_axes>

<!--Display Pref. 0:Hide 1:Wire 3:Flat 4:Shaded Can be overriden for individual
geometries-->

<display_preference>4</display_preference>

</VisibleObject>

<WrapObjectSet>

<objects />

<groups />
```

```
</WrapObjectSet>

</Body>

.

.

.

<PointToPointSpring name="heel_spring_r">

 <!--Flag indicating whether the force is disabled or not. Disabled means that the force is
not active in subsequent dynamics realizations.-->

 <isDisabled>false</isDisabled>

<!--Name of Body to which 1 end of the spring is attached.-->

<body1>tibia_r</body1>

<!--Name of Body to which the 2nd end of the spring is attached.-->

<body2>bottom</body2>

<!--Force application point on body1.-->

<point1> -0.0694 -0.25152 0</point1>

<!--Force application point on body2.-->

<point2> -0.0694 -0.03246 0</point2>

<!--Spring stiffness.-->

<stiffness>50000</stiffness>

<!--Spring resting length.-->
```

```xml
<rest_length>0.14103</rest_length>

</PointToPointSpring>

<PointToPointSpring name="front_spring_r">

<!--Flag indicating whether the force is disabled or not. Disabled means that the force is
not active in subsequent dynamics realizations.-->

<isDisabled>false</isDisabled>

<!--Name of Body to which 1 end of the spring is attached.-->

<body1>tibia_r</body1>

<!--Name of Body to which the 2nd end of the spring is attached.-->

<body2>bottom</body2>

<!--Force application point on body1.-->

<point1> 0.039375 -0.3248643 0</point1>

<!--Force application point on body2.-->

<point2> 0.09117 -0.037503 0</point2>

<!--Spring stiffness.-->

<stiffness>30000</stiffness>

<!--Spring resting length.-->

<rest_length>0.092415</rest_length>

</PointToPointSpring>
```

.

.

.

```xml
<MarkerSet>

<objects>

<Marker name="RTHI">

<!--Body segment in the model on which the marker resides.-->

<body>femur_r</body>

<!--Location of a marker on the body segment.-->

<location> 0 -0.25 0.085</location>

<!--Flag (true or false) specifying whether or not a marker should be kept fixed in the
marker placement step.  i.e. If false, the marker is allowed to move.-->

<fixed>false</fixed>

</Marker>

<Marker name="RKNE">

<!--Body segment in the model on which the marker resides.-->

<body>tibia_r</body>

<!--Location of a marker on the body segment.-->

<location> 0 0 0.075</location>

<!--Flag (true or false) specifying whether or not a marker should be kept fixed in the
marker placement step.  i.e. If false, the marker is allowed to move.-->
```

```
<fixed>false</fixed>

</Marker>

<Marker name="RTIB">

<!--Body segment in the model on which the marker resides.-->

<body>tibia_r</body>

<!--Location of a marker on the body segment.-->

<location> 0 -0.2 0.075</location>

<!--Flag (true or false) specifying whether or not a marker should be kept fixed in the
marker placement step.  i.e. If false, the marker is allowed to move.-->

<fixed>false</fixed>

</Marker>

<Marker name="RANK">

<!--Body segment in the model on which the marker resides.-->

<body>bottom</body>

<!--Location of a marker on the body segment.-->

<location> 0 0 0.075</location>

<!--Flag (true or false) specifying whether or not a marker should be kept fixed in the
marker placement step.  i.e. If false, the marker is allowed to move.-->

<fixed>false</fixed>

</Marker>
```

```xml
<Marker name="RTOE">

<!--Body segment in the model on which the marker resides.-->

<body>bottom</body>

<!--Location of a marker on the body segment.-->

<location> 0.25 -0.09 0</location>

<!--Flag (true or false) specifying whether or not a marker should be kept fixed in the
marker placement step.  i.e. If false, the marker is allowed to move.-->

<fixed>false</fixed>

</Marker>

<Marker name="RHEE">

<!--Body segment in the model on which the marker resides.-->

<body>bottom</body>

<!--Location of a marker on the body segment.-->

<location> -0.1 -0.095 0</location>

<!--Flag (true or false) specifying whether or not a marker should be kept fixed in the
marker placement step.  i.e. If false, the marker is allowed to move.-->

<fixed>false</fixed>

</Marker>

</objects>

<groups />
```

```xml
</MarkerSet>

<!--ContactGeometries  in the model.-->

<ContactGeometrySet>

<objects>

<ContactHalfSpace name="platform">

<!--Body name to connect the contact geometry to-->

<body_name>platform</body_name>

<!--Location of geometry center in the body frame-->

<location>0 0 0</location>

<!--Orientation of geometry in the body frame-->

<orientation>0 0 1.5707</orientation>

<!--Display Pref. 0:Hide 1:Wire 3:Flat 4:Shaded-->

<display_preference>4</display_preference>

</ContactHalfSpace>

<ContactSphere name="heel_r">

<!--Body name to connect the contact geometry to-->

<body_name>bottom</body_name>

<!--Location of geometry center in the body frame-->

<location>-0.05 -0.095 0</location>
```

```xml
<!--Orientation of geometry in the body frame-->

<orientation>0 0 0</orientation>

<!--Display Pref. 0:Hide 1:Wire 3:Flat 4:Shaded-->

<display_preference>4</display_preference>

<radius>0.03</radius>

</ContactSphere>

<ContactSphere name="ball_big_toe_r">

<!--Body name to connect the contact geometry to-->

<body_name>bottom</body_name>

<!--Location of geometry center in the body frame-->

<location>0.171285 -0.1 -0.03</location>

<!--Orientation of geometry in the body frame-->

<orientation>0 0 0</orientation>

<!--Display Pref. 0:Hide 1:Wire 3:Flat 4:Shaded-->

<display_preference>4</display_preference>

<radius>0.02</radius>

</ContactSphere>

<ContactSphere name="small_toe_r">

<!--Body name to connect the contact geometry to-->
```

```
<body_name>bottom</body_name>

<!--Location of geometry center in the body frame-->

<location>0.171285 -0.1 0.04</location>

<!--Orientation of geometry in the body frame-->

<orientation>0 0 0</orientation>

<!--Display Pref. 0:Hide 1:Wire 3:Flat 4:Shaded-->

<display_preference>4</display_preference>

<radius>0.015</radius>

</ContactSphere>

<ContactSphere name="heel_l">

<!--Body name to connect the contact geometry to-->

<body_name>calcn_l</body_name>

<!--Location of geometry center in the body frame-->

<location>0.01 0.01 0.005</location>

<!--Orientation of geometry in the body frame-->

<orientation>0 0 0</orientation>

<!--Display Pref. 0:Hide 1:Wire 3:Flat 4:Shaded-->

<display_preference>4</display_preference>

<radius>0.03</radius>
```

```xml
</ContactSphere>

<ContactSphere name="ball_big_toe_l">

<!--Body name to connect the contact geometry to-->

<body_name>toes_l</body_name>

<!--Location of geometry center in the body frame-->

<location>-0.005 0.005 0.03</location>

<!--Orientation of geometry in the body frame-->

<orientation>0 0 0</orientation>

<!--Display Pref. 0:Hide 1:Wire 3:Flat 4:Shaded-->

<display_preference>4</display_preference>

<radius>0.02</radius>

</ContactSphere>

<ContactSphere name="small_toe_l">

<!--Body name to connect the contact geometry to-->

<body_name>toes_l</body_name>

<!--Location of geometry center in the body frame-->

<location>-0.04 0.005 -0.04</location>

<!--Orientation of geometry in the body frame-->

<orientation>0 0 0</orientation>
```

```
<!--Display Pref. 0:Hide 1:Wire 3:Flat 4:Shaded-->

<display_preference>4</display_preference>

<radius>0.015</radius>

</ContactSphere>

</objects>

<groups />

</ContactGeometrySet>
```

Code credits: Delp S.L., Loan J.P., Hoy M.G., Zajac F.E., Topp E.L., Rosen J.M., Thelen D.G., Anderson F.C., Seth A.

Notes: 3D, 23 DOF gait model created by D.G. Thelen, Univ. of Wisconsin-Madison, and Ajay Seth,

Frank C. Anderson, and Scott L. Delp, Stanford University. Lower extremity joint defintions based on Delp et al. (1990).

Low back joint and anthropometry based on Anderson and Pandy (1999, 2001). Planar knee model of Yamaguchi and Zajac (1989).

Seth replaced tibia translation constraints with a CustomJoint for the knee and removed the patella to eliminate all kinematic constraints; insertions of the quadrucepts are handled with moving points in the tibia frame as defined by Delp 1990.

Anderson reduced number of muscles to improve simulation speed for demonstrations and is not intended to be used in research.

Modification for Right Leg Amputation and prosthetic ankle done by Sandesh G. Bhat (Human Machine Integration Lab, ASU)